EUKARYOTIC CELL, Feb. 2010, p. 251–265 Vol. 9, No. 2
1535-9778/10/$12.00 doi:10.1128/EC.00291-09

Comparative Transcript Profiling of *Candida albicans* and *Candida dubliniensis* Identifies *SFL2*, a *C. albicans* Gene Required for Virulence in a Reconstituted Epithelial Infection Model▽†

Martin J. Spiering,[1]‡ Gary P. Moran,[1] Murielle Chauvel,[2,3] Donna M. MacCallum,[4] Judy Higgins,[1] Karsten Hokamp,[5] Tim Yeomans,[1]§ Christophe d'Enfert,[2,3] David C. Coleman,[1] and Derek J. Sullivan[1]*

Microbiology Research Unit, Division of Oral Biosciences, Dublin Dental School and Hospital, University of Dublin, Trinity College, Dublin 2, Ireland[1]; Institut Pasteur, Unité Biologie et Pathogénicité Fongiques, Paris, France[2]; INRA USC2019, Paris, France[3]; Aberdeen Fungal Group, School of Medical Sciences, Institute of Medical Sciences, University of Aberdeen, Aberdeen AB25 2ZD, United Kingdom[4]; and Smurfit Institute of Genetics, University of Dublin, Trinity College, Dublin 2, Ireland[5]

Received 8 October 2009/Accepted 11 December 2009

***Candida albicans* and *Candida dubliniensis* are closely related species displaying differences in virulence and genome content, therefore providing potential opportunities to identify novel *C. albicans* virulence genes. *C. albicans* gene arrays were used for comparative analysis of global gene expression in the two species in reconstituted human oral epithelium (RHE). *C. albicans* (SC5314) showed upregulation of hypha-specific and virulence genes within 30 min postinoculation, coinciding with rapid induction of filamentation and increased RHE damage. *C. dubliniensis* (CD36) showed no detectable upregulation of hypha-specific genes, grew as yeast, and caused limited RHE damage. Several genes absent or highly divergent in *C. dubliniensis* were upregulated in *C. albicans*. One such gene, *SFL2* (*orf19.3969*), encoding a putative heat shock factor, was deleted in *C. albicans*. ΔΔ*sfl2* cells failed to filament under a range of hypha-inducing conditions and exhibited greatly reduced RHE damage, reversed by reintroduction of *SFL2* into the ΔΔ*sfl2* strain. Moreover, *SFL2* overexpression in *C. albicans* triggered hyphal morphogenesis. Although *SFL2* deletion had no apparent effect on host survival in the murine model of systemic infection, ΔΔ*sfl2* strain-infected kidney tissues contained only yeast cells. These results suggest a role for *SFL2* in morphogenesis and an indirect role in *C. albicans* pathogenesis in epithelial tissues.**

Candida dubliniensis is the closest relative of the important opportunistic human pathogen *Candida albicans* (8, 21, 44). In spite of their close relationship, the two species show significant differences in virulence and epidemiology (42, 43). Although *C. dubliniensis* has historically been associated with oral infections in HIV-infected patients (33), it is generally less pathogenic than *C. albicans*, as judged by differences in carriage rates and prevalence in the human host (7, 27, 28, 45) and by differences in virulence *in vitro* and in murine infection models (8, 12, 23, 41). However, the reasons for these virulence differences are poorly understood and are the focus of investigations to determine their genetic basis.

Among traits important for virulence and variable between *C. albicans* and *C. dubliniensis* are adherence to human epithelial tissues and production of hydrolytic enzymes, as well as resistance to antifungal agents, oxidative stress, and phagocytosis by cells of the host immune system (8, 12, 20, 38, 41, 47). A trait critically important for *Candida* virulence especially in endothelial and epithelial infection models is the ability to undergo the yeast-to-hypha transition (hyphal morphogenesis) (16, 26, 31). Importantly, hyphal morphogenesis in response to many stimuli is consistently slower in *C. dubliniensis* than in *C. albicans* (8, 41). Some specific triggers that induce hyphal morphogenesis in *C. albicans*, such as increased CO_2/HCO_3^- and growth in mammalian tissues (14, 37, 52), do not induce hyphae in *C. dubliniensis* (14, 23, 41). The transcriptional regulator Nrg1 has been identified as a key regulator suppressing filamentation in *C. dubliniensis*, and it has been suggested that this suppression of hyphal growth may partially explain why *C. dubliniensis* is less virulent in the human host than *C. albicans* (23).

The close phylogenetic relationship between *C. albicans* and *C. dubliniensis* may offer opportunities to identify virulence genes in *C. albicans* in infection models where the two species exhibit differences in virulence. A conceptually similar approach, using two *C. albicans* strains differing in their ability to invade tissue in an organ model of mammalian infection coupled with microarray-based analysis of gene expression, identified *DFG16* as being required for pH sensing during tissue invasion (46). The approach adopted in the present study represents a progression from a study by Moran et al. (22), which

* Corresponding author. Mailing address: Microbiology Research Unit, Division of Oral Biosciences, Dublin Dental School and Hospital, University of Dublin, Trinity College, Dublin 2, Ireland. Phone: 353 1 612 7275. Fax: 353 1 612 7295. E-mail: Derek.Sullivan@dental.tcd.ie.

‡ Present address: Center for Advanced Research in Biotechnology, UMBI, Rockville, MD 20850.

§ Present address: Allergy Standards, Ltd., Trinity Enterprise Campus, Dublin 2, Ireland.

† Supplemental material for this article may be found at http://ec.asm.org/.

▽ Published ahead of print on 18 December 2009.

TABLE 1. *Candida* strains used in this study

Strain	Description	Parent strain	Source or reference
C. albicans			
SC5314	Wild type		9
CaMS1	Δ*orf19.4445*::*SAT1*/*orf19.4445*	SC5314	This study
CaMS1-1	Δ*orf19.4445*::*FRT*/*orf19.4445*	CaMS1	This study
CaMS16	Δ*orf19.4445*::*FRT*/Δ*orf19.4445*::*SAT1*	CaMS1-1	This study
CaMS24	Δ*orf19.7304*::*SAT1*/Δ*orf19.7304*::*SAT1*	SC5314	This study
CaMS24-2	Δ*orf19.7304*::*FRT*/Δ*orf19.7304*::*FRT*	CaMS24	This study
CaMS46	Δ*SFL2*::*SAT1*/*SFL2*	SC5314	This study
CaMS48	Δ*SFL2*::*SAT1*/*SFL2*	SC5314	This study
CaMS46-2	Δ*SFL2*::*FRT*/*SFL2*	CaMS46	This study
CaMS48-2	Δ*SFL2*::*FRT*/*SFL2*	CaMS48	This study
CaMS49	Δ*SFL2*::*FRT*/Δ*SFL2*::*SAT1*	CaMS46-2	This study
CaMS49-1	Δ*SFL2*::*FRT*/Δ*SFL2*::*FRT*	CaMS49	This study
CaMS50	Δ*SFL2*::*FRT*/Δ*SFL2*::*SAT1*	CaMS46-2	This study
CaMS50-1	Δ*SFL2*::*FRT*/Δ*SFL2*::*FRT*	CaMS50	This study
CaMS58	Δ*SFL2*::*FRT*/*SFL2*::*SAT1*	CaMS49-1	This study
CaMS60	Δ*SFL2*::*FRT*/*SFL2*::*SAT1*	CaMS50-1	This study
CEC955	*ura3*Δ::λ *imm434*/*ura3*Δ::λ *imm434 his1*::*hisG*/*HIS1 arg4*::*hisG*/*ARG4 ADH1*/*adh1*::(*ADH1p-cartTA SAT1 TETp-caGFP*)	BWP17	A. Firon and C. d'Enfert, unpublished
CEC1352	*ura3*Δ::λ *imm434*/*ura3*Δ::λ *imm434 his1*::*hisG*/*HIS1 arg4*::*hisG*/*ARG4 ADH1*/*adh1*::(*ADH1p-cartTA SAT1 TETp-caGFP*) *RPS1*/*RPS1*::(*URA3 TETp-SFL2*)	CEC955	This study
CEC1147	*ura3*Δ::λ *imm434*/*ura3*Δ::λ *imm434 his1*::*hisG*/*HIS1 arg4*::*hisG*/*ARG4 ADH1*/*adh1*::(*ADH1p-cartTA SAT1 TETp-caGFP*) *RPS1*/*RPS1*::(*URA3 TETp-GFP*)	CEC955	A. Firon and C. d'Enfert, unpublished
C. dubliniensis			
CD36	Wild type		44
Wü284	Wild type		24
CD36/pNIM1GFP	*ADH1*/*adh1*::(*ADH1p-cartTA SAT1 TETp-caGFP*)	CD36	This study
CD36/pNIM1SFL2	*ADH1*/*adh1*::(*ADH1p-cartTA SAT1 TETp-caSFL2*)	CD36	This study
Wü284/pNIM1GFP	*ADH1*/*adh1*::(*ADH1p-cartTA SAT1 TETp-caGFP*)	Wü284	This study
Wü284/pNIM1SFL2	*ADH1*/*adh1*::(*ADH1p-cartTA SAT1 TETp-caSFL2*)	Wü284	This study

analyzed the genome contents of *C. albicans* and *C. dubliniensis* by comparative genomic hybridization to *C. albicans* gene arrays. Although the vast majority of genes are highly conserved between the two species, approximately 200 *C. albicans* genes (representing ~4.0% of its genome) are absent or highly diverged in *C. dubliniensis*, including known virulence genes and genes of unknown function (11, 22). Availability of the genome sequences of *C. albicans* (4, 13) and *C. dubliniensis* (11) in database-accessible formats (2, 11) has enabled mining of the differences in the genetic repertoire of the two species.

For comparative study of *C. albicans* and *C. dubliniensis* gene expression, a suitable human infection model has to fulfill several criteria: chiefly ease of use, reproducibility, and sufficient recovery of fungal material for analysis. Reconstituted human oral epithelium (RHE) represents such a model, having been used extensively to study *Candida* virulence (reviewed in reference 36), including microarray-based transcriptional profiling (52). The RHE infection model permits quantitative measurements of virulence, and we have recently demonstrated that *C. dubliniensis* is far less virulent than *C. albicans* in the RHE model (23, 41). Here we report the results of gene expression profiling in *C. albicans* and *C. dubliniensis* coincubated with RHE tissue, representing the first comparative analysis of global transcription in these two species in an infection model. We further describe the identification of one *C. albicans* gene, which we have named *SFL2* (*orf19.3969*; IPF8627.2), which is critical for filamentation *in vitro* and virulence in the RHE model.

MATERIALS AND METHODS

Strains and culture conditions. The *C. albicans* and *C. dubliniensis* strains used in this study are listed in Table 1. Growth media were from Oxoid (Basingstoke, Hampshire, United Kingdom), and amino acids were from Sigma-Aldrich Ireland, Ltd. (Tallaght, Dublin, Ireland). All strains were cultured on yeast extract-peptone-dextrose (YPD) agar or in YPD broth at 37°C and 200 rpm, unless indicated otherwise. All liquid media for fungal cell cultures for microarray studies or in transformation experiments were filter sterilized. Hexose solutions (10× concentration) used in agar media were filter sterilized and added to molten agar media shortly before pouring.

Chemicals and enzymes. All chemicals used were analytical grade or molecular biology grade and supplied by Sigma-Aldrich, Ambion (Warrington, United Kingdom), or Roche Diagnostics (Mannheim, Germany). Ultrapure Milli-Q water (Millipore Ireland B.V., Cork, Ireland) was used in all experiments. PCRs for cloning of DNA constructs were performed with Expand high-fidelity enzyme (Roche), and diagnostic PCRs were carried out with GoTaq enzyme (Promega, Madison, WI).

RHE inoculation and coincubation with *Candida* cells and RHE tissue damage measurements. Inoculation and coincubation of RHE with *Candida* cells were performed as previously described (41). In brief, *Candida* cells were grown in semisynchronized cultures (i.e., in 25°C and 37°C serial YPD cultures) (36) and harvested by centrifugation, the cell density was adjusted in phosphate-buffered saline (PBS), and RHE tissues were inoculated as described previously (41). *Candida* cultures on polycarbonate filter (PCF) membranes (used as RHE support matrix) were initiated in the same way as the RHE cultures. *Candida* RHE and *Candida* PCF cultures and RHE-only controls were incubated in MCDB 153 maintenance medium (containing 0.1% glucose; Skinethic Laboratories, Nice,

TABLE 2. Primers used in this study

Name	Sequence (5′→3′)
CdADH1 F1	TCCCCGCGGTTGAGATGAGACCGT[a]
CdADH1 R1	GCTCTAGACATAATTGTTTTTGTATTTG[b]
M13F/5′orf19.3969	AGTATAGAAATTTTTTCCATATCTTTCCAATTAGTACAACCATTCCTACAATTAATCTACCT ATTCAGTTTTGATTTCCGGTAAAACGACGGCCAGT
M13F/5′orf19.7304	TACTCTTGCTTCCCCTCCCTACTCTTGCTTCCCCTCCCTACTCTTACTCCCCCTCCCTACTCCA TTCCACCAACCACTTAGTAAAACGACGGCCAGT
M13F/orf19.3969complR	GATACTGATAATATGAATAAATGATGTTGTATAATATATAGAGTTTTATTGTATTAGAATT TTTCAATATAAAATAAAAAGTAAAACGACGGCCAGT
M13F/orf19.4445R1	CCATTCACCACTAGAACAAGTATCAGTAAAACGACGGCCAGT
M13R/3′orf19.3969	AGCTAGTTGAAGAAATTAAAAAGTTATATCTCTCCCTCTATAATCTTTGTTCATATTTCTTA GTTATCTCTCTATACGTTGGAAACAGCTATGACCATG
M13R/orf19.4445F2	CAGAGAATCAGCAACGCGCTATTGGAAACAGCTATGACCATG
M13R/3′orf19.7304	TGAAATCAATGATAAATTGTTAAAAAAATATGCATAACTTCACAACTAATCACCACCACTA CTACTTAATAATACCCTTCGGAAACAGCTATGACCATG
Nourse-split1	GATTGATCTGTCGGCAGTGGTTTC
Nourse-split2	CAAATTCGATGAGACTGTGCGCGA
orf19.3969complF	AGTATAGAAATTTTTTCCATATCTTTCCAATTAGTACAACCATTCCTACAATTAATCTACCT ATTCAGTTTTGATTTCCG
orf19.3969complR/M13F	ACTGGCCGTCGTTTTACTTTTTATTTTATATTGAAAAATTCTAATACAATAAAACTCTATAT ATTATACAACATCATTTATTCATATTATCAGTATC
orf19.3969GTWF	GGGACAAGTTTGTACAAAAAAGCAGGCTTGATGAGTAAGAAAAATCCTGGTGATCCTCGT
orf19.3969GTWR	GGGACCACTTTGTACAAGAAAGCTGGGTTTTATTCATATTATCAGTATCATCATCACT
orf19.4445F1	GAATGTTGGAAGTAGTCGAAATCGTG
orf19.4445F1nest	CCGTGTTAAATGTGTGGATCCTATTGCC
orf19.4445F2/M13R	CATGGTCATAGCTGTTTCCAATAGCGCGTTGCTGATTCTCTG
orf19.4445R1/M13F	ACTGGCCGTCGTTTTACTGATACTTGTTCTAGTGGTGAATGG
orf19.4445R2	TAACCCACACAAAACACAGCCAAC
orf19.4445R2nest	GGTGTATCCCAACTCGTGCAATTCCTG
qP-ACT1F	AGCTCCAGAAGCTTTGTTCAGACC
qP-ACT1R	TGCATACGTTCAGCAATACCTGGG
qP-Cd36_54430F	GCAACCACTACAACAACCGCTACA
qP-Cd36_54430R	CTGGTGGTGCCGGTATTTGTTGAA
qP-orf19.7304F	GGTCCAATTGTCATTGGTATTGGCA
qP-orf19.7304R	AATAGCCACGCATGCACCATTGGA
qP-RPS7ACalbF	GTTGCTCAAGCTTTCGTTGATTTGG
qP-RPS7ACdubF	GTTGCTCAAGCTTTTGTTGATTTGG
qP-RPS7AR	GCTTGTAAACTTGGTGGTGGAACG
qP-SFL2F	CCACACCAACAACCAGAAATGGCT
qP-SFL2R	TGTTGGACAGTAGACCCAGGTTGT
SAT1check1	AATCCAGACAGTCGAGTTAGACAGA
SAT1check2	GAGCACAGGATGACGCCTAACAT
SFL2 F2	GACCTGTCGACGCAACAATGAGTAAGAAAAATCC[c]
SFL2 R2	TGAAGATCTTCATTTATTCATATTATCAGTATCA[d]

[a] The SacII restriction site is underlined.
[b] The XbaI restriction site is underlined.
[c] The SalI restriction site is underlined.
[d] The BglII restriction site is underlined.

France) in a CO_2 incubator at 37°C, with 5% (vol/vol) CO_2 and 100% humidity, and sampled for RNA or lactate dehydrogenase (LDH) measurements (see below) at regular time points (30, 90, 360, or 720 min). Activity of human LDH in RHE culture medium was measured with the CytoTox 96 nonradioactive cytotoxicity assay (Promega) (41). The LDH assay product, formazan, was measured by spectrophotometry, and concentrations were determined with its extinction coefficient (15,600 M^{-1} cm^{-1}). *Candida* RHE cultures and RHE controls (0.5 cm^2) were fixed, sectioned, stained, and examined by light microscopy as previously described (41). Cell morphology in *Candida* PCF cultures was examined by light microscopy of cell suspensions obtained by rinsing the PCF membranes.

RNA extraction. For RNA extractions, 2 ml of a solution containing 2 parts (vol/vol) RNA*later* solution (Ambion) and 1 part filter-sterilized 10% (wt/vol) saponin (Sigma-Aldrich) in PBS was added to a 4-cm^2 *Candida* RHE or *Candida* PCF culture. To recover the fungal cells, membranes were rinsed 3 or 4 times with the RNA*later*-saponin solution, and the cell suspensions from 2 or 3 *Candida* RHE or *Candida* PCF cultures were transferred to a 50-ml centrifuge tube (Sarstedt, Wexford, Ireland) along with the cut filter membranes and immediately frozen and stored at −20°C. For total RNA extraction, cell suspensions containing the filter membranes were thawed at room temperature, vortexed for 5 to 10 s, and centrifuged (3,200 × *g* for 5 min). The membranes were removed, the tubes were centrifuged as before, and the supernatant was removed by careful aspiration. RNA was extracted with the RNeasy minikit (Qiagen, West Sussex, United Kingdom) with cell disruption performed in a Mikro-Dismembrator S system (Sartorius Stedim Biotech, Göttingen, Germany) for 2 min at 2,000 rpm. *Candida* cultures (~8 ml) used as the 0-min control (inoculum) in PBS (described above) were harvested by centrifugation as before, taken up in 2 ml RNA*later* solution, and stored at −20°C; RNA was extracted from *Candida* cell pellets as described above. Total RNA was resuspended in nuclease-free water and DNase I treated with the DNA*free* Turbo kit (Ambion), measured by 260/280 spectrophotometer readings, and integrity was checked on 1.2% Tris-borate-EDTA (TBE) gels. Absence of DNA in RNA samples after DNase treatment was routinely checked by PCR with primers qP-ACT1F and qP-ACT1R (Table 2).

Amplification and Cy labeling of RNA and hybridization to *Candida* gene arrays. The Amino Allyl MessageAmp II aRNA amplification kit (Ambion) was used for RNA amplification and labeling, following the manufacturer's protocol. One microgram of total RNA was used for reverse transcription, and amino-allyl-labeled RNA (aaRNA) was linearly amplified by T7-based *in vitro* transcription (49). aaRNA was Cy labeled with *N*-hydroxysuccinimide esters of Cy3 and

Cy5 dyes (GE Healthcare, Bucks, United Kingdom) and used in hybridizations to *C. albicans* gene arrays. *Candida albicans* 70-mer oligoarrays (NRC, Canada) representing 6,320 open reading frames (ORFs) spotted in duplicate on glass slides were used in gene expression profiling of *C. albicans* or *C. dubliniensis* RHE cultures 30 min postinoculation (p.i.) versus inoculum cultures (0 min). These experiments were carried out in 3 biological replicates (fresh RHE and *Candida* cultures set up on separate occasions) with dye swaps performed on biological replicates. *C. albicans*-spotted cDNA gene arrays (Eurogentec, Seraing, Belgium) representing 6,039 ORFs were used in expression profiling of *Candida* RHE cultures 90 min p.i., relative to *Candida* PCF cultures 90 min p.i., performed in two biological replicates with dye swaps carried out within each replicate. Approximately 5 μl of Cy-labeled aaRNA (1 μg of each treatment) was incubated at 70°C for 5 min, chilled on ice for 1 min, added to 55 μl digoxigenin (DIG) EasyHyb solution (Roche Diagnostics), and immediately loaded onto a microarray slide in a hybridization chamber (Corning, NY). Slides were covered with a plastic HybriSlip (Schleicher & Schuell, Keene, NH), incubated stationary in a hybridization oven at 42°C for 16 to 18 h, and washed in 50-ml washing solutions at room temperature. The following washes were performed: 10 min with 1× SSC (0.15 M NaCl plus 0.015 M sodium citrate) plus 0.2% SDS, 10 min with 0.1× SSC plus 0.2% SDS, and 5 min with 0.1× SSC. Slides were briefly dipped in fresh 0.1× SSC and sterile Milli-Q water, dried by centrifugation at 500 × *g*, and scanned immediately.

Microarray data analysis. Microarray slides were scanned with a GenePix 4000B scanner (Axon Instruments, Sunnyvale, CA) at a resolution of 10 μm, using the auto PMT setting. Fluorescent intensity data were extracted using GenePix Pro 6.1 software (Axon Instruments). GenePix result (gpr) files were uploaded into ArrayPipe (http://www.pathogenomics.ca/arraypipe/) (10) for further analysis. Log_2-transformed ratios of Cy5 to Cy3 intensities were calculated for each detected feature, effects of background subtraction and normalization methods were assessed with MA plots, and variation among technical replicates were assessed by interslide ratio plots. Analysis settings giving normal distribution of intensity ratios and acceptable variation among replicates were background subtraction with the normexp algorithm (35) and loess normalization on each subgrid. To identify consistently expressed genes, only those genes whose expression was detected in at least 2 biological replicates were included in further analysis. Statistical significance of differences in log_2 ratios from 0 (no change) within groups was determined with empirical Bayes (eBayes) moderated one-sample *t* tests (39) and between groups by two-sample Student's *t* tests.

Sequence retrieval and analyses. Genomic, exon-only, and predicted protein sequences were retrieved from the *Candida* Genome database (http://www.candidagenome.org/) or *Candida dubliniensis* GeneDB (http://www.genedb.org/genedb/cdubliniensis/) for *C. albicans* (Assembly 21) and *C. dubliniensis*, respectively, and used in primer design for real-time PCR and PCR-based cloning and for BLAST searches. Real-time PCR primers were designed in SciTools at IDT (http://www.idtdna.com/SciTools/SciTools.aspx?c = US) using the default settings; wherever possible, the length of PCR products was restricted to 80 to 150 bp. Primers were purchased from Sigma-Aldrich.

Extraction of fungal genomic DNA. *Candida* genomic DNA for PCR-based cloning, diagnostic PCR, or quantitative PCR (qPCR) was extracted as described previously (40) with modifications. To a cell pellet from a 2-ml overnight culture in a 1.5-ml microcentrifuge tube was added 12 acid-washed glass beads (0.7 to 1 mm; Sigma-Aldrich) and 0.3 ml lysis buffer (40 mM Tris-acetate, 20 mM sodium acetate, 1 mM EDTA, 1% SDS [pH 7.8]); the mixture was vortexed for 1 min and incubated for 30 to 45 min at 65°C, and DNA was extracted as described previously (40).

RT and qPCR for quantitative analysis of gene expression. Primers used in real-time quantitative PCR (qPCR) are listed with prefix "qP" in Table 2. Reverse transcription (RT) was performed with 250 ng of total RNA, 0.05 μM gene-specific primer, and Superscript II reverse transcriptase (Invitrogen, Carlsbad, CA) in 10-μl volumes following the manufacturer's protocol. Reverse transcription real-time qPCR (RT-qPCR) for quantification of gene expression was carried out with Power or Fast Sybr green kits (Applied Biosystems, Foster City, CA), with 25 μl containing 0.4 μM each primer and the ABI 7700 sequence detector or the ABI 7500 Fast real-time PCR system (Applied Biosystems). Each reaction was carried out in duplicate. Cycling conditions were 1 hold at 95°C for 10 min and 40 cycles of 95°C for 30 s, 50°C for 30 s, and 70°C for 1 min. Amplification efficiency of each gene primer set was determined with 7 serial DNA concentration steps (within 0.1 to 100 ng of genomic DNA). All primer sets had amplification efficiencies that were not significantly different from that for the endogenous control gene, *ACT1* ($P > 0.05$; extra-sum-of-squares *F* test of regression slopes in GraphPad Prism 4.0c; GraphPad Software, Inc.; http://www.graphpad.com/prism/Prism.htm).

As found in previous studies (6), *ACT1* expression varied among different growth conditions, but its variability was lower than that of *PMA1* and *TFB4*, also evaluated as normalizing genes (M.J.S., unpublished observation). To account for the variation in *ACT1* expression in the normalization of gene expression, the variation in *ACT1* expression among nine treatments (inoculum cultures, as well as RHE and PCF cultures at four time points) was quantified with equally loaded RNA. Threshold cycle (C_T) values for *ACT1* obtained from two independent experiments carried out in three technical replicates were used to calculate an adjustment factor (AF) for each treatment (TR) by the equation $AF_{ACT1(TR)} = 2^{C_T\ ACT1(TR)\ -\ C_T\ ACT1(median)}$, where $C_{T\ ACT1(TR)}$ is the C_T for *ACT1* in the treatment and $C_{T\ ACT1(median)}$ is the median C_T of *ACT1* of the 9 treatments. AF values were calculated for each *C. albicans* and *C. dubliniensis* and *ACT1*-normalized and AF-adjusted expression (= normalized expression [NE]) of a test gene (*G*) in each treatment determined from the C_T s for *G* and for *ACT1* by the equation $NE_{G(TR)} = 2^{-[C_T\ G(TR) - C_T\ ACT1(TR)]} \times AF_{ACT1(TR)}{}^{-1}$.

***Candida* gene knockout constructs.** Gene knockout (ko) constructs for *orf19.7304* and *SFL2* (*orf19.3969*) were generated by a PCR-based method (50). The *SAT1* flipper cassette (34) was PCR amplified from M13 forward and reverse priming sites in plasmid pSFS2A, with primers having 80 bases at their 5′ ends that were identical to the 5′ upstream or 3′ downstream regions, respectively, of the targeted gene. PCR amplification was with primers M13F/5′ orf19.3969 and M13R/3′ orf19.3969 to replace *SFL2* and M13F/5′ orf19.7304 and M13R/3′ orf19.7304 to replace *orf19.7304* with the *SAT1* flipper. All PCRs were performed in 50-μl reaction mixtures, using a cycling regimen of 1 hold at 95°C for 2 min and then 7 cycles of 95°C for 30 s, 58°C for 30 s, and 70°C for 4 min followed by 28 cycles of 95°C for 30 s and 68°C for 5 min. *orf19.4445* was deleted by a split-marker approach. Its 5′- and 3′-flanking regions were PCR amplified from SC5314 genomic DNA with primers orf19.4445F1 and orf19.4445R1/M13F and orf19.4445F2/M13R and orf19.4445R2, respectively. Partial, overlapping *SAT1* cassettes were generated by PCR with pSFS2A and primers M13F/orf19.4445R1 and Nourse-split2 and primers Nourse-split1 and M13R/orf19.4445F2. The 5′ and 3′ *orf19.4445* flanks were fused to the partial *SAT1* cassettes in a thermocycler reaction (1 cycle of 95°C for 2 min and then 10 cycles of 95°C for 30 s and 70°C for 5 min), followed by PCR with primers orf19.4445F1nest and Nourse-split2 (*orf19.4445* 5′-flanking region with a 3.8-kb *SAT1* fragment) or primers orf19.4445R2nest and Nourse-split2 (*orf19.4445* 3′-flanking region with the 0.9-kb *SAT1* fragment). The amplified deletion constructs were purified with the GeneElute PCR clean-up kit (Sigma) and concentrated by ethanol precipitation. DNA pellets (2 to 5 μg) were taken up in 5 μl sterile ultrapure water for transformation.

***Candida* transformation and confirmation of transformant genotypes.** *Candida* cells were transformed by electroporation as previously described (23) and selected on YPD plates with 200 μg/ml nourseothricin (Jena Bioscience GmbH, Jena, Germany). Correct integration of *SAT1* into the targeted gene locus was checked with primers SAT1check1 or SAT1check2 and primers annealing outside the gene region targeted for knockout.

C. albicans is diploid; therefore, the two alleles of each gene were removed by sequential deletion, utilizing the reusable *SAT1* flipper marker (34). The number of alleles in heterozygous and homozygous ko and complemented strains was checked by qPCR with genomic DNA (1 ng per 20-μl reaction) and the applicable "qP" primers (Table 2) annealing within the gene regions targeted for deletion, using the same reagents and instrumentation as described for RT-qPCR. Amplification of *ACT1* was used as a normalizing control for loading, and wild-type (WT) SC5314 was used as the calibrator for determination of the number of alleles in each transformant.

Complementation of *SFL2*-deleted transformants. To reintroduce *SFL2* into Δ*sfl2* strains, the *SFL2* ORF was amplified from SC5314 genomic DNA by PCR (35 cycles of 95°C for 30 s and 68°C for 3 min) with primers orf19.3969complF containing 80 bases with 100% identity to the region immediately upstream of the deleted *SFL2* region and orf19.3969complR/M13F, containing 80 bases 100% identical to the *SFL2* 3′ untranscribed region (UTR) gene region—deleted in Δ*sfl2* strains—and M13F sequence in reverse complement orientation. The *SAT1* cassette was PCR amplified as before with primers M13F/orf19.3969complR and M13R/3′ orf19.3969, containing 80 bases 100% identical to the intergenic region immediately downstream of the deleted *SFL2* 3′ UTR region. Both fragments were targeted to the *SFL2* locus *via* the 80-nucleotide-long *SFL2*-flanking sequences; the 98-bp sequence overlapping the *SFL2* fragment with the *SAT1* cassette was absent in the Δ*sfl2* strains and permitted *in vivo* recombination between the two fragments. The two DNA fragments were purified as described above, mixed in equimolar amounts to give 2 to 5 μg DNA in 5 μl, and used to transform *Candida* cells. Transformants were selected by nourseothricin resistance, and reintroduction of *SFL2* was checked by PCR and qPCR as described above.

***SFL2* overexpression in *C. albicans* and expression in *C. dubliniensis*.** An *SFL2* overexpression vector for *C. albicans* was constructed using Gateway cloning tech-

nology (Invitrogen). The *SFL2* ORF devoid of its stop codon was amplified from *C. albicans* genomic DNA using primers orf19.3969GTWF and orf19.3969GTWR and a cycling regimen of 1 hold at 95°C for 3 min and then 7 cycles of 94°C for 15 s, 52°C for 15 s, and 72°C for 2.5 min followed by 26 cycles of 94°C for 15 s, 60°C for 15 s, and 72°C for 2.5 min. The PCR product was cloned in the pDONR207 vector using the Gateway BP clonase (Invitrogen) according to the supplier's instructions. Using Gateway LR clonase (Invitrogen), the *SFL2* ORF was then transferred into the CIp-Op2 expression vector, a derivative of CIp10 (25) that harbors a doxycycline-inducible promoter (30) and a Gateway cloning cassette (A. Firon and C. d'Enfert, unpublished results). A control plasmid was constructed using the ORF for green fluorescent protein (GFP). The resulting *SFL2* and GFP overexpression plasmids were linearized with StuI to promote targeting at the *C. albicans RPS1* locus and transformed into *C. albicans* strain CEC955, yielding strains CEC1352 and CEC1147, respectively.

To express Ca*SFL2* in *C. dubliniensis* strains CD36 and Wü284, the following procedure was used. Plasmid CdpNIM1 was produced by replacing the *C. albicans* 5′ *ADH1* DNA sequence in pNIM1 (30) with the orthologous *C. dubliniensis ADH1* sequence, obtained by PCR using the primers CdADH1 F1 and CdADH1 R1 (which contain SacII and XbaI restriction enzyme sites, respectively). The 3′ *ADH1* sequence was left unchanged in pNIM1, because it is highly similar in *C. dubliniensis*. This plasmid was then digested with SalI and BglII to replace the GFP-coding sequence with the *SFL2* (*orf19.3969*) ORF (containing SalI and BglII cutting sites on either end), PCR amplified from *C. albicans* SC5314 using primers SFL2 F2 and SFL2 R2. The resulting CdpNIM1SFL2 construct and the GFP control, CdpNIM1, were linearized with SacII and KpnI for electroporation into CD36 or Wü284. Transformants were screened by PCR for the presence of *SFL2* (CD36/pNIM1SFL2 and Wü284/pNIM1SFL2) or GFP (CD36/pNIM1GFP and Wü284/pNIM1GFP), and maintained on YPD containing 100 μg/ml nourseothricin.

Phenotypic analysis of gene deletion strains *in vitro* and *in vivo*. For germ tube induction tests, *Candida* cells were grown in YPD overnight at 30°C or 37°C and inoculated into 10% (vol/vol) fetal calf serum (FCS) in water (41). Germ tubes were identified by light microscopy at a 400× magnification as filaments nonconstricted at the septa. To generate microaerophilic conditions, cells were grown in YPD overnight at 30°C with shaking (200 rpm) and collected by centrifugation. Approximately 100 cells in 5 μl PBS were added to 50 μl of yeast extract–2% sucrose (YPSuc) liquid agar (2%; cooled to 50°C), spotted on 10 ml YPSuc agar, overlaid with 15 ml YPSuc agar, and grown for 24 to 48 h at 25°C or 37°C. Spider and Pal's agar media were prepared as described previously (1, 18), and cells were incubated at 30°C or 37°C for 5 days. The effects of a pH shift on morphology were tested by using cells precultured overnight in liquid Lee's medium (15) at pH 4.5 and 30°C, which were diluted 1:500 into fresh Lee's medium at pH 6.5 and 37°C.

C. albicans morphological responses to CO_2 were tested by adding cells from an overnight YPD shaking culture (200 rpm) grown at 37°C to give a density of 2×10^6 cells/ml in 25 ml yeast nitrogen base (YNB) medium (Sigma-Aldrich) with 0.1% glucose and an amino acid mixture based on the composition of artificial saliva (51). Cells were then incubated in static cultures at ambient (0.038%) or 5% CO_2 at 37°C and examined by light microscopy. To test the sensitivity of gene knockouts and the WT to specific stresses, they were grown in YPD broth at 30°C to mid-exponential phase, and 10-fold serial dilutions of these cells spotted onto YPD plates and YPD plates supplemented with either 1 M NaCl or 5 mM H_2O_2. Growth was monitored after 24 and 48 h at 30°C (42°C for the heat shock assay).

Virulence of deletion mutants in the mouse systemic model of infection was measured as described previously (23). For each fungal strain, six female BALB/c mice (6 to 8 weeks old) (Harlan, United Kingdom) were inoculated intravenously with 1.2×10^4 to 1.4×10^4 cells/g of body weight and survival was monitored over 28 days. Mice were humanely terminated when they had lost 20% body weight, showed signs of distress, or were no longer able to freely access food and water. Kidneys, spleen, and brain were removed from culled mice, and fungal burdens were determined by homogenizing tissues in sterile saline and plating on YPD agar to determine viable cell counts. In a second experiment, for each strain, five female BALB/c mice were inoculated intravenously with 2.8×10^4 to 3.2×10^4 cells/g of body weight. Mice were culled on day 3 postinfection, and kidneys, liver, lung, spleen, and brain were sampled for fungal organ burdens. In both infection models, half of each kidney was also fixed in formalin, to allow paraffin sections to be produced. Kidney sections (5 μm) were stained by Grocott's methenamine silver stain and poststained with light-green SF yellowish stain, or periodic acid Schiff stained with hematoxylin poststaining.

Microarray data accession numbers. Raw and processed microarray data have been submitted to GEO (http://www.ncbi.nlm.nih.gov/geo/) under accession no. GSE13318 and GSE13345.

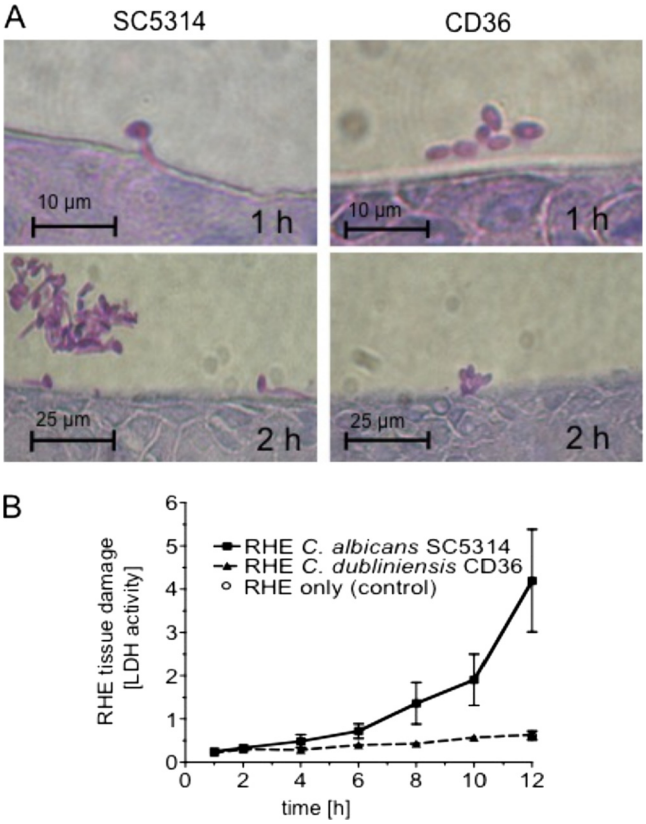

FIG. 1. Growth morphology and tissue damage by *C. albicans* SC5314 and *C. dubliniensis* CD36 on RHE. Growth on RHE 1 to 2 h p.i. (A) and RHE tissue damage (measured as LDH activity released from RHE *Candida* cultures) by the two species 1 to 12 h p.i and in uninoculated RHE 12 h p.i. (B). (Note that the data point for the uninoculated control is largely obscured by the value for CD36, because the two values are essentially identical.) LDH data were normalized to the mean formazan concentration of all treatments (mean ± 1 SE; $n = 3$ to 5). The difference in levels of LDH release 12 p.i. between SC5314 and CD36 was statistically significant ($P < 0.01$; Mann-Whitney test).

RESULTS

***Candida albicans* and *Candida dubliniensis* show major differences in growth morphology very early during RHE infection.** As shown previously, *C. albicans* is more virulent in the RHE infection model than *C. dubliniensis* because *C. dubliniensis* is unable to form hyphae in this model (23, 41). These earlier studies focused on RHE colonization ≥12 h postinoculation (p.i.) when differences in hyphal formation were most apparent. To identify genes involved in the very early stages of this morphological switch in *C. albicans*, we conducted a time course study of RHE infection to determine the time points at which the differences in growth morphology between the two species first became evident. To this end, RHE tissues were inoculated with *C. albicans* SC5314 or *C. dubliniensis* CD36, incubated in 5% CO_2 at 37°C, and sampled at regular time points 1 to 12 h postinoculation for tissue histology and to measure RHE tissue damage (41). *C. albicans* cells had begun to form germ tubes by 1 h p.i., whereas *C. dubliniensis* cells grew in the yeast phase (Fig. 1A), in which they remained for the whole duration of the experiment (12 h). These results

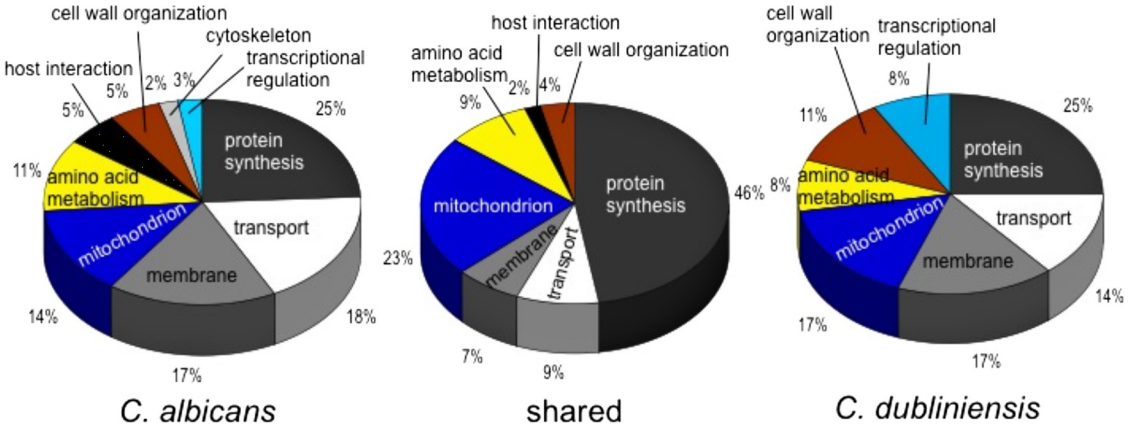

FIG. 2. Functional categories of the genes showing significant upregulation in *C. albicans* and *C. dubliniensis* in RHE 30 min p.i. relative to 0 min (control). Biological categories of the upregulated genes were assigned with CGD's Gene Ontology Slim Mapper (http://www.candidagenome.org/cgi-bin/GO/goTermMapper).

indicated that major differences in growth morphology between *C. albicans* and *C. dubliniensis* occurred within 1 h of RHE colonization. RHE tissue damage (measured as LDH activity release into the RHE medium) by *C. albicans* started to increase within 4 to 12 h p.i., while damage of RHE tissues inoculated with *C. dubliniensis* was identical to that in the uninfected control (Fig. 1B).

***C. albicans*, but not *C. dubliniensis*, shows early upregulation of virulence genes on RHE.** The above results suggested that significant differences in gene expression underlying the morphological differences between the two species may already be present within <1 h of RHE colonization. Therefore, we chose 30 min p.i., at which time the vast majority of cells grew as yeast (data not shown) for comparative analysis of global gene expression with whole-genome microarrays. Total RNA was extracted from cells of both species on RHE 30 min p.i. and from the 0-min reference controls (*Candida* cells from the same cell pools used to inoculate the RHE; see Materials and Methods). Cy-labeled amplified RNAs (aaRNAs) from *C. albicans* or *C. dubliniensis* RHE cultures 30 min p.i. were cohybridized with aaRNAs from the respective 0-min control cultures to *C. albicans* oligonucleotide microarrays (NRC, Canada). In three biological replicates, 2,654 and 1,301 consistently expressed genes were identified in *C. albicans* and *C. dubliniensis*, respectively.

To identify genes highly expressed in both species in the RHE, the following selection criteria were applied: ≥2-fold upregulation in RHE 30 min p.i. and statistically significant ($P < 0.05$; eBayes t test) difference from 1 (no change in expression). This yielded 268 genes (10.1% of all expressed genes) in *C. albicans* and 82 (6.3%) genes in *C. dubliniensis*, with 47 genes upregulated in both species (see Tables S1 and S2 in the supplemental material). The majority of upregulated genes in the two species fell into the categories of protein synthesis, cellular transport, membrane, amino acid metabolism, or mitochondrial genes (Fig. 2). The array probes contained *C. albicans* sequences; so given some sequence divergence between *C. albicans* and *C. dubliniensis* genes (11, 22), detection of fewer expressed genes in *C. dubliniensis* was expected. To distinguish between lack of detection due to sequence divergence and that due to absence of expression in *C. dubliniensis*, we estimated the minimum sequence identity between probe and target sequences for detection of expression in *C. dubliniensis* by using the array probe sequences for all genes (shown in Tables S1 and S2 in the supplemental material) in BLASTN searches of *C. dubliniensis* GeneDB (http://www.genedb.org/genedb/cdubliniensis/blast.jsp). The majority of genes (76%) showing consistent expression in *C. dubliniensis* had probe-target similarities of ≥90% along ≥68 nucleotides (see Table S2 in the supplemental material), indicating that this level of probe-target similarity permitted reliable detection of expression of *C. dubliniensis* genes with the *C. albicans* oligoarray.

Ribosomal protein genes were the largest group showing upregulated expression in RHE 30 min p.i.: 83 (30% of all upregulated genes) and 37 (44%) ribosomal protein genes were ≥2-fold upregulated in *C. albicans* and *C. dubliniensis*, respectively (see Tables S1 and S2 in the supplemental material). RT-qPCR confirmed the expression for two ribosome-biogenesis genes in both species: *RPS7A*, whose dynamics in increase of expression were very similar to those of the hyphally regulated *C. albicans* gene *ECE1* (Fig. 3A) and those of *NOP1* (Fig. 3B) in both species. Gene expression profiles were consistent with the respective morphologies of the two species in the RHE. Even at this early stage, *C. albicans* exhibited upregulation of several hyphally regulated and virulence-associated genes, including *ECE1*, *HWP1*, *HYR1*, *ALS3*, *IHD1*, and *RBT1* (see Table S1 in the supplemental material), encoding hypha-specific proteins or cell surface adhesins, commonly upregulated in human tissue models (32, 46, 52). With the exception of *IHD1*, probes for all of these genes had <90% similarity to *C. dubliniensis* sequences, and no upregulated expression of any hyphally regulated genes was detectable in *C. dubliniensis*, with the exception of one gene, *NIP7*, encoding a hyphally induced ribosomal protein (see Table S2 in the supplemental material). The *C. albicans* gene set was also significantly enriched for genes encoding protein mannosyltransferases: i.e., *PMT1*, *PMT2*, *PMT4*, and *PMT6* were >2-fold upregulated in *C. albicans*, but not in *C. dubliniensis* (sequence similarity to the *PMT* gene probes was >90%, except for being 89% for

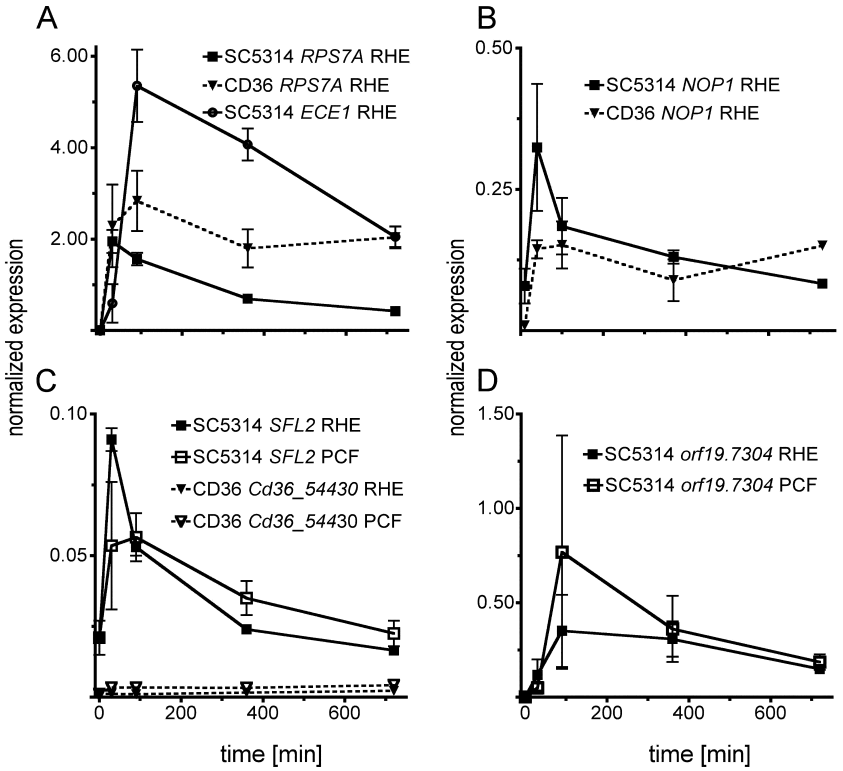

FIG. 3. Expression of *RPS7A*, *ECE1*, and *NOP1* and genes absent from or divergent in *C. dubliniensis* 0 to 12 h p.i. on RHE or PCF. (A) Expression of *RPS7A* in *C. albicans* and *C. dubliniensis* and *ECE1* in *C. albicans* on RHE; (B) expression of *NOP1* in *C. albicans* and *C. dubliniensis* on RHE; (C) expression of *SFL2* in *C. albicans* and of its likely orthologue, *Cd35_54430*, in *C. dubliniensis* on RHE and PCF; and (D) expression of *orf19.7304* in *C. albicans* on RHE and PCF. Expression of genes was measured by RT-qPCR, and all data were normalized to *ACT1* expression. Data are not plotted to the same scale; values are means ± SE ($n = 2$).

PMT4 [see Table S1 in the supplemental material]). The numbers of genes showing significant ($P < 0.05$) and ≥2-fold-downregulated expression in the RHE were 176 (6.6% of all expressed genes) for *C. albicans* and 49 (1.9%) for *C. dubliniensis*, with 16 genes showing significant downregulation in both species. The majority (>50%) of downregulated genes had unknown functions, and several encoded enzymes for intra- and extracellular metabolite transport (ABC transport proteins as well as peptide and hexose transporters [see Tables S3 and S4 in the supplemental material]).

Besides interactions with epithelial cells in the RHE tissue, other factors in the RHE environment, including CO_2 levels and microaerophilic conditions, could affect morphology and gene expression in the *Candida* cells. Therefore, to control for these conditions (29), we also grew *C. albicans* and *C. dubliniensis* on the polycarbonate filters (PCF) used as support matrix for the RHE. *C. albicans*—but not *C. dubliniensis*—formed hyphal elements when incubated on the polycarbonate filters under the same conditions and in the same growth medium as the RHE cultures (not shown). To profile gene expression, cells of each *Candida* species were incubated on RHE or PCF for 90 min. aaRNAs from RHE and PCF cultures were cohybridized to Eurogentec's *C. albicans* cDNA array, and in two biological replicates, consistent expression of 4,613 genes for *C. albicans* and 1,368 genes for *C. dubliniensis* was detected. In total, 222 (4.8%) genes in *C. albicans* (see Table S5 in the supplemental material) and 122 (8.9%) genes in *C. dubliniensis* (see Table S6 in the supplemental material) showed significantly ($P < 0.05$) and ≥1.5-fold upregulated expression on RHE 90 min p.i. relative to PCF 90 min p.i.

There were 78 genes that displayed upregulation on RHE relative to PCF in both species (35% and 64% of all upregulated in genes in *C. albicans* and *C. dubliniensis*, respectively). Among these were several heat shock protein genes (i.e., *HSP12*, *HSP60*, *HSP70*, *HSP78*, and *HSP104* [see Tables S5 and S6 in the supplemental material]), suggesting similarities in stress response in the two species. Also upregulated in both species were genes encoding enzymes for utilization of C_2 compounds (i.e., fatty acid β-oxidation, glyoxylate cycle, and gluconeogenesis), such as *POX1-3*, *ICL1*, and *PCK1*, which was confirmed by RT-qPCR analysis (data not shown).

***C. albicans* shows early upregulation of several genes absent or divergent in *C. dubliniensis*.** Following the initial characterization of the *C. albicans* and *C. dubliniensis* gene sets, we focused on uncharacterized genes that may be absent from or divergent in *C. dubliniensis* (22), as increased expression of these genes in *C. albicans* in the RHE may provide clues to their possible involvement in *Candida* virulence in this model. In this analysis, genes were preselected based upon ≥1.5-fold upregulation ($P < 0.05$) in *C. albicans* and on expression significantly different from expression in *C. dubliniensis* ($P < 0.05$; Student's *t* test). In the RHE experiment 30 min p.i. versus the 0-min experiment, 146 genes fulfilled these criteria (data not shown), 20 of which had unknown functions and 3 of which

TABLE 3. *C. albicans* genes of unknown function or with divergent orthologues in *C. dubliniensis* showing significant[a] and ≥1.5-fold upregulation in *C. albicans* in RHE 30 min p.i.

Gene common name[b]	*C. albicans* systematic name	*C. dubliniensis* closest putative homologue systematic name	% Sequence identity to probe (length of alignment [bp])[c]	Product description	Normalized expression in[d]:				
					C. albicans SC5314		*C. dublinienis* CD36		
					Fold change	eBayes *t* test *P* value[e]	Fold change	eBayes *t* test *P* value[e]	Student's *t* test *P* value[f]
IPF16210	*orf19.1782*	*Cd36_24080*	0	Unknown function	4.79	0.0034	ND	NA	NA
*HWP1**	*orf19.1321*	*Cd36_43360*	46 (64)	Hyphal wall protein	4.74	0.0135	ND	NA	NA
IPF22064	*orf19.5136*	*Cd36_72830*	93 (70)	Unknown function	3.45	0.0076	ND	NA	NA
IPF24039	*orf19.3266*	*Cd36_25930*	88 (70)	Unknown function	3.07	0.0039	ND	NA	NA
IPF22684	*orf19.4590*	*Cd36_41920*	97 (63)	Unknown function	2.46	0.0008	ND	NA	NA
*HYR1**	*orf19.4975*	*Cd36_51670*	0	GPI[g]-anchored putative cell wall protein	2.39	0.0041	ND	NA	NA
IPF22235	*orf19.5009*	*Cd36_12710*	89 (69)	Unknown function	2.35	0.0050	ND	NA	NA
IPF24177	*orf19.3142*	*Cd36_46140*	91 (70)	Unknown function	2.19	0.0084	ND	NA	NA
IPF17436	*orf19.4600.1*	*Cd36_41810*	96 (56)	Unknown function	2.18	0.0155	−1.30	0.0551	0.0349
IPF26752	*orf19.556*	*Cd36_30580*	96 (69)	Unknown function	1.95	0.0011	1.10	0.3595	0.0230
IPF18467	*orf19.3394*	*Cd36_62010*	90 (70)	Unknown function	1.94	0.0113	ND	NA	NA
IPF8627*	*orf19.3969*	*Cd36_54430*	0	Predicted HSF-type DNA-binding protein	1.93	0.0026	ND	NA	NA
IPF24338	*orf19.2995*	*Cd36_02840*	87 (70)	Unknown function	1.91	0.0196	ND	NA	NA
IPF26046	*orf19.1287*	*Cd36_53740*	93 (43)	Unknown function	1.90	0.0183	ND	NA	NA
IPF25066	*orf19.2259*	*Cd36_21320*	88 (70)	Unknown function	1.89	0.0395	ND	NA	NA
IPF15822	*orf19.2457*	*Cd36_05580*	90 (62)	Unknown function	1.86	0.0166	ND	NA	NA
IPF18322	*orf19.3141*	*Cd36_46150*	95 (65)	Unknown function	1.86	0.0229	ND	NA	NA
IPF20385	*orf19.6748*	*Cd36_87330*	90 (70)	Unknown function	1.60	0.0275	ND	NA	NA
IPF19812*	*orf19.7304*	*Cd36_34500*	79 (67)	Unknown function	1.60	0.0112	ND	NA	NA
IPF14519	*orf19.4703*	*Cd36_34320*	0	Unknown function	1.60	0.0252	ND	NA	NA
IPF23019	*orf19.4241*		0	Unknown function	1.59	0.0177	ND	NA	NA
IPF3432	*orf19.6177*	*Cd36_87690*	84 (70)	Unknown function	1.57	0.0103	ND	NA	NA
IPF24748	*orf19.2558*	*Cd36_26640*	0	Unknown function	1.54	0.0482	ND	NA	NA
IPF25503	*orf19.1829*	*Cd36_73360*	0	Unknown function	1.53	0.0496	ND	NA	NA

[a] Statistically significant upregulation of expression (eBayes *t* test; $P < 0.05$) in *C. albicans.*
[b] *, absent from or divergent in *C. dubliniensis* (22).
[c] Percent sequence identity of 70-mer probes on *C. albicans* oligoarray (NRC, Canada) to *C. dubliniensis* orthologue sequences. Identity was determined by BLASTN. The length of the longest alignment with the probe is given in parentheses where applicable.
[d] Genes are ordered from highest to lowest fold changes in expression in *C. albicans*. ND, not detected; NA, not applicable.
[e] Fold change ≠ 1.
[f] Significant difference in fold change between *C. albicans* and *C. dubliniensis*.
[g] GPI, glycosylphosphatidylinositol.

were predicted to be absent or very divergent in *C. dubliniensis* (Table 3). One of these genes, *HYR1*, encoding a hyphal cell wall protein, showed ≥2-fold upregulation in *C. albicans* in RHE. The other two, *orf19.3969* (IPF8627) and *orf19.7304* (IPF19812), had only predicted or unknown functions, respectively. Because of sequence relationships with *SFL1* described below, we assigned *orf19.3969* the name "*SFL2*."

In the RHE-PCF 90-min p.i. comparison, we identified 24 genes with unknown function that were predicted to be absent from or divergent in *C. dubliniensis* (10.8% of all upregulated genes in *C. albicans*) and that had ≥1.5-fold upregulation on the RHE relative to PCF in *C. albicans* (Table 4). Among these genes was *HYR1*, also upregulated in RHE 30 min p.i. relative to 0 min (see above), while *SFL2* was not among the genes showing differential expression in RHE relative to PCF 90 min p.i. (confirmed by RT-qPCR analysis) (Fig. 3), suggesting similar regulation of this gene under the two conditions.

RT-qPCR confirmed very early upregulation of *SFL2* after inoculation onto RHE. *C. albicans SFL2* was >3-fold increased ($P < 0.05$; *t* test) 30 min p.i. compared to expression at 0 min and declined 90 to 720 min p.i.: *SFL2* expression was also upregulated in cells grown on PCF 30 min p.i., but tended to be lower than expression in RHE 30 min p.i. (Fig. 3). The putative *SFL2* orthologue in *C. dubliniensis*, *Cd36_54430*, identified based on both sequence homology and synteny (in the *Candida* Genome Database) (2), showed no appreciable increase in expression under any condition, and its expression levels appeared to be more than 1 order of magnitude lower than expression of *C. albicans SFL2*. Expression of *orf19.7304* in *C. albicans* increased rapidly within 90 min on both RHE and PCF, with a gradual decline approximately 360 to 720 min p.i. (Fig. 3).

***SFL2* is required for *C. albicans* filamentation in response to multiple environmental signals.** Upregulated expression of *SFL2* (*orf19.3969*) and *orf19.7304* in the RHE suggested their possible involvement in *C. albicans* virulence. BLAST alignments of the predicted protein sequences for *SFL2* with its closest *C. dubliniensis* orthologue, *Cd36_54430*, and *orf19.7304* with its closest orthologue, *Cd36_34500*, indicated only 50% identity (58% similarity) and 68% identity (78% similarity) between them, respectively. Therefore, we focused on *SFL2* and *orf19.7304* for functional analysis by targeted gene knockout. Also included in these tests was *orf19.4445*, as its expression increased in *C. albicans* upon transfer to the RHE (not shown) and was 3-fold greater than expression on PCF 90 min p.i. (Table 4).

TABLE 4. *C. albicans* genes of unknown function or with divergent orthologues in *C. dubliniensis* with significant[a] and ≥1.5-fold upregulation in *C. albicans* on RHE relative to expression on PCF 90 min p.i.

Gene common name[b]	*C. albicans* systematic name	*C. dubliniensis* closest putative homologue systematic name	% Sequence identity to probe (length of alignment [bp])[c]	Product description	Normalized expression in[d]:				
					C. albicans SC5314		*C. dublinienis* CD36		
					Fold change	eBayes *t* test *P* value[e]	Fold change	eBayes *t* test *P* value[e]	Student's *t* test *P* value[f]
IPF4032	*orf19.6168*	*Cd36_80830*	75 (300)	Predicted spindle pole body component	3.21	0.0000	ND	NA	NA
IPF8957	*orf19.4894*	*Cd36_09640*	92 (326)	Unknown function	3.21	0.0000	1.45	0.0088	0.0298
IPF3092	*orf19.4445*	*Cd36_06760*	85 (325)	Unknown function	3.03	0.0000	ND	NA	NA
*HYR1**	*orf19.4975*	*Cd36_51670*	57 (357)	GPI[g]-anchored putative cell wall protein	2.95	0.0000	ND	NA	NA
IPF4696	*orf19.5282*	*Cd36_11100*	86 (381)	Unknown function	2.72	0.0001	ND	NA	NA
IPF12799	*orf19.2515*	*Cd36_81030*	89 (280)	Unknown function	2.35	0.0007	ND	NA	NA
IPF1548	*orf19.951*	*Cd36_50410*	72 (251)	Unknown function	1.90	0.0042	ND	NA	NA
*POL93**	*orf19.6078*		0	Predicted gypsy-like reverse transcriptase	1.86	0.0091	ND	NA	NA
IPF7182	*orf19.3439*	*Cd36_61560*	86 (268)	Unknown function	1.78	0.0082	ND	NA	NA
IPF15784	*orf19.715*	*Cd36_32010*	83 (342)	Unknown function	1.70	0.0025	ND	NA	NA
IPF13890*	*orf19.4918*	*Cd36_44430*	0	Unknown function	1.69	0.0015	ND	NA	NA
IPF7456	*orf19.2047*	*Cd36_15710*	88 (322)	Unknown function	1.67	0.0046	ND	NA	NA
IPF12629	*orf19.5552*	*Cd36_63350*	92 (366)	Unknown function	1.67	0.0057	ND	NA	NA
IPF13017	*orf19.1785*	*Cd36_24050*	71 (259)	Unknown function	1.65	0.0021	ND	NA	NA
IPF18468	*orf19.4467*	*Cd36_03660*	93 (327)	Unknown function	1.61	0.0173	ND	NA	NA
IPF3468*	*orf19.4055*		0	Unknown function	1.60	0.0027	ND	NA	NA
IPF4704	*orf19.5278*	*Cd36_11140*	88 (281)	Unknown function	1.60	0.0038	ND	NA	NA
IPF10005	*orf19.6196*	*Cd36_06620*	84 (306)	Unknown function	1.59	0.024	ND	NA	NA
IPF11796	*orf19.2791*	*Cd36_07020*	90 (329)	Unknown function	1.57	0.0047	ND	NA	NA
IPF22331	*orf19.5026*	*Cd36_12870*	88 (328)	Unknown function	1.57	0.0034	ND	NA	NA
IPF13231*	*orf19.3877*	*Cd36_31750*	74 (302)	Predicted LPF family protein	1.56	0.0152	ND	NA	NA
IPF11858	*orf19.1277*	*Cd36_45480*	87 (273)	Unknown function	1.54	0.0041	ND	NA	NA
IPF12435*	*orf19.5619*	*Cd36_63710*	75 (290)	Predicted LPF family protein	1.52	0.0100	ND	NA	NA
IPF19617	*orf19.1350*	*Cd36_22460*	75 (279)	Unknown function	1.51	0.0105	ND	NA	NA

[a] Statistically significant upregulation of expression (eBayes *t* test; $P < 0.05$) in *C. albicans.*
[b] *, absent from or divergent in *C. dubliniensis* (22).
[c] Percent sequence identity of cDNA probes on *C. albicans* gene arrays (Eurogentec) to *C. dubliniensis* orthologue sequences. Identity was determined by BLASTN. The length of the longest alignment with the probe is given in parentheses where applicable.
[d] Genes are ordered from highest to lowest fold changes in expression in *C. albicans*. ND, not detected; NA, not applicable.
[e] Fold change ≠ 1.
[f] Significant difference in fold change between *C. albicans* and *C. dubliniensis.*
[g] GPI, glycosylphosphatidylinositol.

SFL2, *orf19.7304*, and *orf19.4445* were deleted separately in SC5314 by replacement of each gene with the *SAT1* flipper cassette (34). Several heterozygous (Δ) and homozygous (ΔΔ) knockout (ko) strains were generated (Table 1), and their phenotypes were tested in a range of filamentation-inducing conditions. Deletion of *orf19.7304* and *orf19.4445* had no detectable effects on cell morphology in 10% fetal calf serum (FCS) and embedded growth in agar (not shown) and were not investigated any further in this study. However, cells of the Δ*sfl2* and ΔΔ*sfl2* ko strains displayed filamentation defects under several conditions. When cells of the ΔΔ*sfl2* ko strains were precultured at 30°C in YPD and inoculated into 10% FCS and incubated at 37°C, they formed germ tubes at a rate similar to the wild type (WT) (data not shown). However, in the absence of a temperature shift (37°C preculture), germ tube formation in the ΔΔ*sfl2* strains was reduced by approximately 50% and 7% compared to that in the WT after incubation in 10% serum for 30 min and 45 min, respectively.

SFL2 ko mutants were also impaired in hyphal formation in response to a pH shift. Following a shift from pH 4.5 to pH 6.5 in Lee's liquid medium, after 3 h of incubation, approximately 80% of WT cells had produced germ tubes or true hyphae, whereas Δ*sfl2* cells exhibited only 10 to 20% germ tube formation, and ΔΔ*sfl2* cells failed entirely to form hyphae in response to this pH shift (data not shown). Reintroduction of a WT *SFL2* allele into the ΔΔ*sfl2* strains restored filamentation to levels similar to those of the heterozygous Δ*sfl2* strains (data not shown).

We then tested morphological responses to increased CO_2, which induces hyphae in *C. albicans* (14, 37). To detect CO_2-specific morphogenic responses, we used a YNB medium with 0.1% glucose and supplemented with amino acids (YNB-Gluc-AA [see Materials and Methods]) in which the WT formed germ tubes only in 5% CO_2 and not in ambient CO_2 (Fig. 4). In YNB-Gluc-AA and 5% CO_2, the Δ*sfl2* strain formed fewer and less-elongated germ tubes than the WT, the ΔΔ*sfl2* strain did not form any germ tubes, and the ΔΔ*sfl2* strain with reintroduced *SFL2* showed germ tube formation similar to that of the Δ*sfl2* strain.

We next tested the morphological responses of the mutant strains to microaerophilic conditions that induce filamentation in *C. albicans* (5). Cells were embedded in YPSuc agar and incubated at 25°C or 37°C; identical results were obtained at

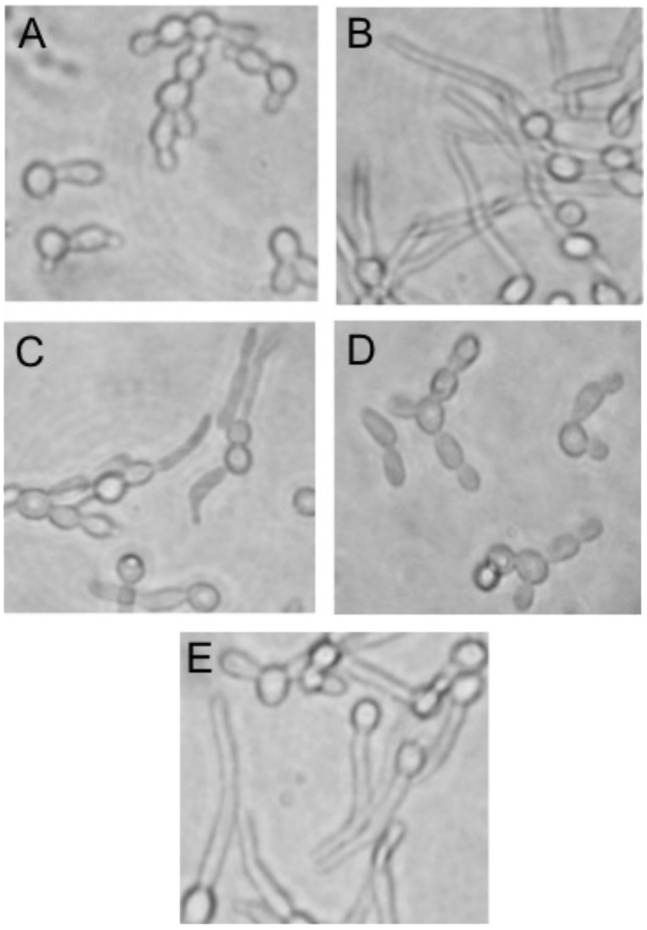

FIG. 4. Growth of *C. albicans SFL2* knockout and complemented strains under high-CO_2 conditions. Shown are cells of wild-type strain SC5314 in ambient (0.038%) CO_2 (A) and 5% CO_2 (B) and cells of the Δ*sfl2* strain (CaMS46-2) (C), ΔΔ*sfl2* strain (CaMS49-1) (D), and ΔΔ*sfl2* strain with reintegrated *SFL2* (CaMS58) (E) in modified YNB medium after 3 h of growth in 5% CO_2 at 37°C.

both temperatures, and only results for embedded growth at 37°C are shown. The WT strain formed long elongated filaments (Fig. 5A and B). In contrast, only 20% of Δ*sfl2* colonies produced some filaments, and all ΔΔ*sfl2* colonies were completely smooth and formed only short chains of yeast cells or pseudohyphae. Reintroduction of the *SFL2* wild-type allele into the ΔΔ*sfl2* strain restored hyphal formation to a level similar to that of the Δ*sfl2* strain.

When incubated on Pal's agar at 30°C for <72 h, *C. albicans* grows as smooth colonies; however, when grown at 37°C for >72 h, it forms smooth colonies with a hyphal fringe (D.J.S., unpublished data). Following growth for 96 h at 37°C on Pal's agar, wild-type SC5314 formed colonies with a hyphal fringe, as expected, whereas ΔΔ*sfl2* colonies lacked a hyphal fringe (Fig. 5C). On Spider agar, the wild-type strain formed wrinkled colonies with a hyphal fringe (data not shown), while the Δ*sfl2* strain exhibited wrinkled colonies without a fringe and the ΔΔ*sfl2* strain grew as fringeless, completely smooth colonies. The ΔΔ*sfl2* strain complemented with a wild-type copy of *SFL2* formed wrinkled colonies on Spider agar that were similar to those of the Δ*sfl2* strain (data not shown).

Deletion of *SFL2* had no detectable effect on growth under aerobic conditions in standard media: the doubling time of the ΔΔ*sfl2* strain during mid-log phase (60 to 330 min) in YPD at 37°C was 60.6 ± 2.1 min (median ± standard error [SE]; $n = 2$) and essentially identical to that of the parental WT strain (60.8 ± 2.7 min). Growth of ΔΔ*sfl2* cells in response to heat, salt, or oxidative stress was similar to that of the WT (data not shown).

Overexpression of *SFL2* from a doxycycline-inducible promoter in *C. albicans* resulted in the formation of filaments in liquid YPD at 30°C, while the control (expressing GFP from the same promoter) grew only as yeast (Fig. 6). Moreover, when the *SFL2*-overexpressing strain CEC1352 was grown on solid YPD or YPD plus 1% FCS at 37°C, colonies appeared wrinkled, whereas the colonies of the GFP-overexpressing strain remained smooth. Expression of Ca*SFL2* in *C. dubliniensis* CD36 or Wü284 under the control of the doxycycline-inducible promoter and grown in YPD and doxycycline resulted in elongated cells and pseudohy-

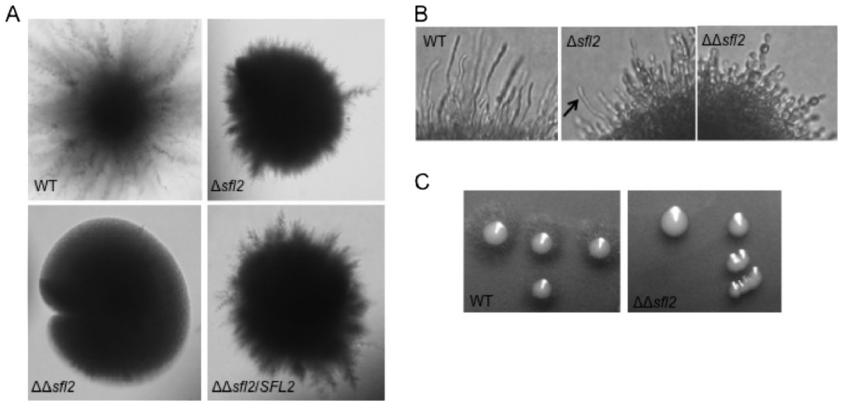

FIG. 5. Growth morphologies of *C. albicans* SC5314 and *SFL2* deletants under agar-embedded (microaerophilic) conditions. (A) Colonies of the WT strain, Δ*sfl2* strain (CaMS46-2), ΔΔ*sfl2* strain (CaMS49-1), and ΔΔ*sfl2* strain with reintegrated *SFL2* (ΔΔ*sfl2*/*SFL2* [CaMS58]) grown in YPSuc agar for 48 h at 37°C; (B) closeups of the WT strain, Δ*sfl2* strain (CaMs46-2; a hyphal element is indicated by the arrow), and ΔΔ*sfl2* strain (CaMs50-1) in YPSuc agar for 24 h at 37°C; and (C) colony morphology of the WT and ΔΔ*sfl2* (CaMs50-1) strains on Pal's agar after 96 h of growth at 37°C.

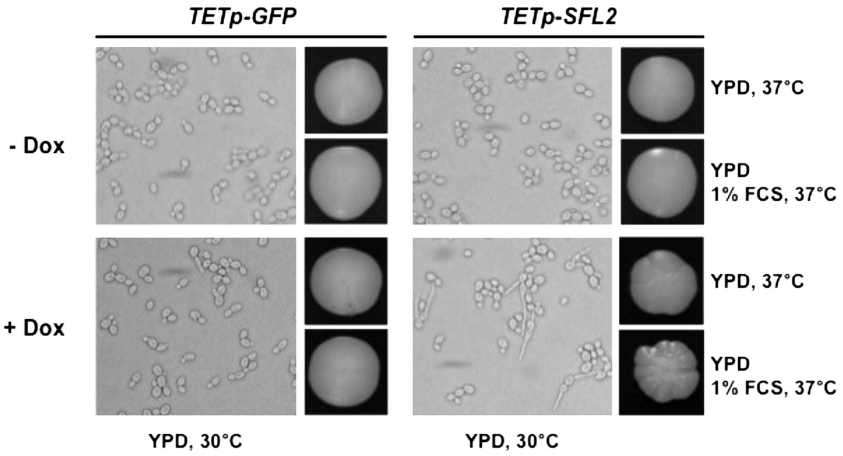

FIG. 6. Overexpression of *SFL2* in *C. albicans*. Strains CEC1352 (Table 2; indicated by *TETp-SFL2*), overexpressing *SFL2* from a doxycycline-inducible promoter, and CEC1147 (Table 2; indicated by *TETp-GFP*), expressing GFP from a doxycycline-inducible promoter, were grown for 18 h in liquid YPD at 30°C or for 5 days on solid YPD or YPD plus 1% FCS at 37°C in the presence or absence of doxycycline (50 μg/ml).

pha-like elements, whereas the GFP-expressing strains grew solely as yeast cells (data not shown).

***SFL2* is required for RHE tissue colonization and damage by *C. albicans*, but not for virulence in the mouse model of systemic infection.** To see if *SFL2* deletion affected colonization and tissue damage to the RHE, the *SFL2* ko strains were tested in this model. Compared to the WT, which exhibited extensive filamentation in the RHE, the Δ*sfl2* strain showed only few hyphal elements, and cells of the ΔΔ*sfl2* strains were completely impaired in hyphal morphogenesis in the RHE; ΔΔ*sfl2* strains with reintegrated *SFL2* showed filamentation levels similar to those of the Δ*sfl2* strain (Fig. 7). RHE damage mirrored the morphological phenotypes: i.e., sequential deletion of each *SFL2* allele resulted in a gradual reduction of tissue damage: LDH release caused by Δ*sfl2* strains was approximately 40% of that of the WT, and LDH release by ΔΔ*sfl2* strains was about 50% of LDH release by Δ*sfl2* strains and significantly lower than that of the WT ($P < 0.01$; analysis of variance [ANOVA] and Tukey's test), with RHE damage similar to that in the uninfected control. RHE damage by ΔΔ*sfl2* strains with reintegrated *SFL2* was similar to that of the Δ*sfl2* strains.

Finally, we tested ΔΔ*sfl2* strains in *in vivo* mouse models of systemic infection, using the conventional 28-day model and a 3-day infection model. In these experiments, virulence of the ΔΔ*sfl2* strain CaMS49-1 was very similar to that in the WT: survival times of mice inoculated with ΔΔ*sfl2* or WT (SC5314) cells were 16.7 ± 3.9 and 15.3 ± 2.9 days (mean ± SE; $n = 6$), respectively ($P > 0.05$; Kaplan-Meier and log rank statistics), with no significant differences ($P > 0.05$; ANOVA) detected for *Candida* burdens in the kidney, spleen, or brain (data not shown). To examine whether changes in organ burdens were evident at an earlier time point during infection, mice were infected and then sampled at 3 days postinfection. Again, there was no significant difference in *Candida* burdens for the kidney, lung, liver, spleen, and brain (data not shown). Interestingly, histology of kidney sections obtained from the 3- and 28-day infection models revealed that the ΔΔ*sfl2* strain was defective in hypha formation, growing almost exclusively as yeast cells

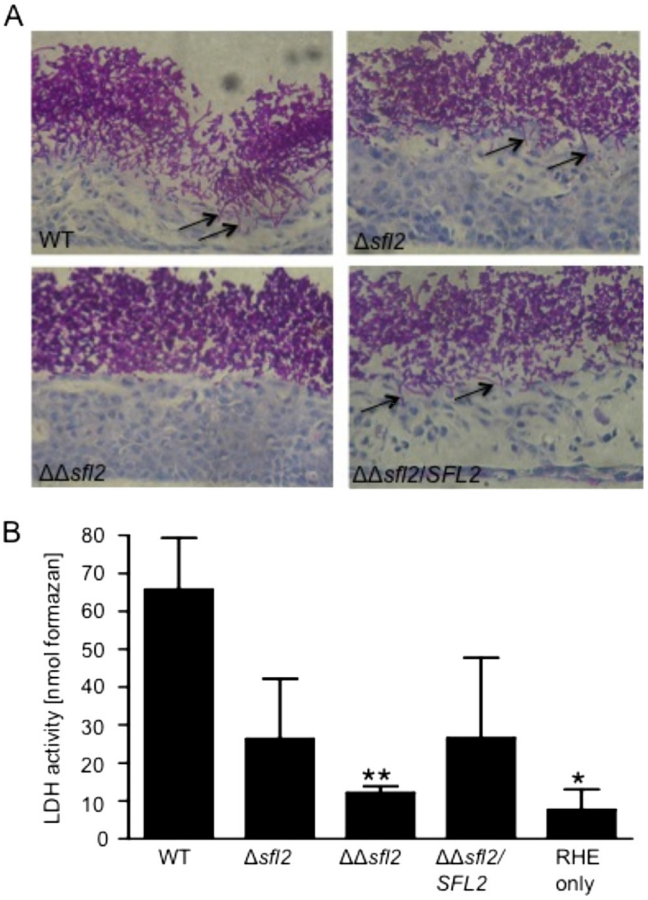

FIG. 7. Growth morphology and tissue damage by *C. albicans SFL2* knockout and complemented strains in RHE. (A) Growth morphology in RHE 33 h p.i. Hyphal elements present in SC5314 (WT) and the Δ*sfl2* and ΔΔ*sfl2*/*SFL2* strains are indicated by arrows. (B) RHE tissue damage, measured as LDH release (means ± SE; $n = 2$ to 4) 25 h p.i., by the WT and heterozygous (Δ) and homozygous (ΔΔ) *sfl2* strains (CaMS48-2 and CaMS49-1, respectively) and the complemented ΔΔ*sfl2* strain (CaMS60). One-way ANOVA detected a significant ($P = 0.011$) effect on LDH release; Tukey's test detected significant differences in LDH release between the WT and ΔΔ*sfl2* strains and the RHE-only control, indicated by asterisks (*, $P < 0.05$; **, $P < 0.01$).

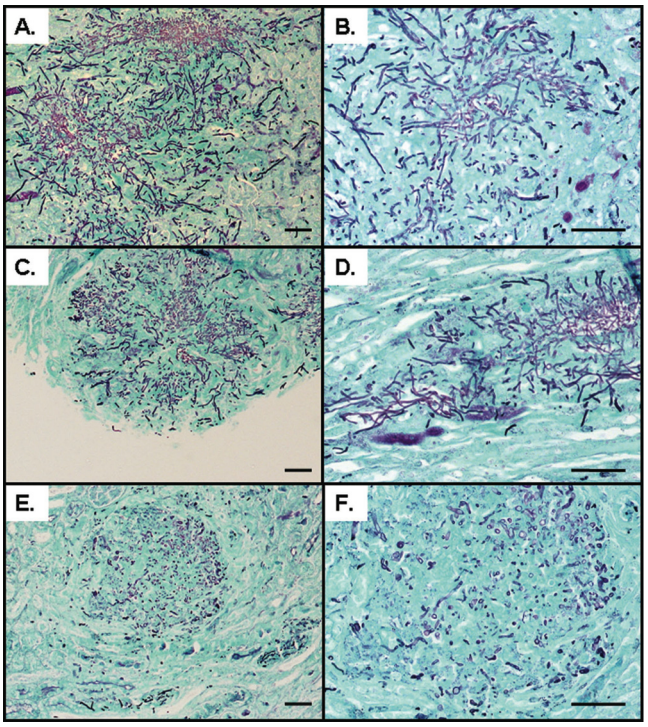

FIG. 8. Morphology of *C. albicans SFL2* knockout strains in mouse kidneys. Kidney sections (5 μm; 3 days postinfection) were stained with methenamine silver and poststained with light green. The photographs shown represent two different magnifications. Panels A and B show the WT strain, panels C and D show the Δ*sfl2* strain, and panels E and F show the ΔΔ*sfl2* strain. Bars, 50 μm.

with only a few short filaments (Fig. 8). Consistent with the *in vitro* phenotypes, Δ*sfl2* strain-infected renal lesions showed an intermediate phenotype, with some lesions containing long hyphae and others containing short filaments or yeasts (Fig. 8).

***SFL2* encodes a putative DNA-binding heat shock factor protein.** BLASTP searches of the NCBI nonredundant (nr) protein database with the inferred Sfl2p sequence (714 amino acids) gave a significant match with Hsr1p (E = 1e−51, 64% identity; alignment of 129 amino acids at the Sfl2p protein N terminus), described as a heat-shock-related transcription factor (HSF) in *Candida tropicalis* (CAC12663), and WU-BLAST2 searches of *Saccharomyces cerevisiae* YeastDB (at http://seq.yeastgenome.org) gave significant (E < 1e−18) matches to several HSF-type proteins, including Sfl1p (19 to 62% identity) and Mga1p (25 to 28% identity). A highly conserved HSF-type DNA-binding domain (pfam00447; E = 6e−16) and an HSF-type DNA-binding domain signature (PS00434; at amino acids 57 to 81) were detected in the N-terminal region of Sfl2p, also present at the same location (amino acids 58 to 82) in its putative *C. dubliniensis* orthologue, Cd36_54430p. Sfl2p shared about 24% identity and the HSF-type signature with its closest relative in *C. albicans*, Sfl1p (*orf19.454*), which is a negative regulator of hyphal morphogenesis (3, 17).

DISCUSSION

The opportunistic pathogens *C. albicans* and *C. dubliniensis* have a close phylogenetic relationship and share several morphophysiological traits. Despite this, they display large differences in virulence, with *C. albicans* being much more pathogenic in the human host and in human infection models than *C. dubliniensis*. Here, to identify novel virulence-associated genes in *C. albicans* and begin to characterize commonalities and differences in gene expression between the two species, we compared global gene expression in *C. albicans* and *C. dubliniensis* in the RHE model of the oral mucosa. Both species exhibited coordinated upregulation of primary metabolism genes in RHE 30 min postinoculation, indicating conserved responses in general metabolism in the two species. However, whereas *C. albicans* showed rapid filamentation and caused increased RHE tissue damage, as well as upregulated expression of several known hyphally regulated genes, *C. dubliniensis* grew only as yeast cells, caused very limited RHE damage, and lacked detectable upregulation of hyphal genes. *C. albicans* also displayed upregulation of several genes of unknown function that were absent or significantly divergent in *C. dubliniensis*. One such gene, *SFL2* (*orf19.3969*), showed significant upregulation in *C. albicans* on the RHE 30 min p.i. and high (~50%) sequence divergence with its likely orthologue in *C. dubliniensis* (*Cd36_54430*). When *SFL2* was deleted in *C. albicans*, cells were unable to form hyphae under a variety of conditions, including growth under microaerophilic or high-CO_2 conditions, in response to pH shifts, and in mouse kidneys. Overexpression of *SFL2* resulted in increased filamentation in *C. albicans* and the production of pseudohypha-like cells in *C. dubliniensis*. Deletion of *SFL2* in *C. albicans* had no effect on mouse survival in the systemic infection model; however, *SFL2* deletion led to decreased RHE colonization and damage, demonstrating a possible role for *SFL2* in virulence in this oral mucosal infection model.

The greater virulence of *C. albicans* and the limited virulence of *C. dubliniensis* were consistent with earlier observations (12, 41) and with lower carriage and prevalence of *C. dubliniensis* in the oral cavities of healthy individuals (42, 43). *C. albicans* and *C. dubliniensis* displayed broadly similar patterns of coordinately upregulated expression of ribosomal and other primary metabolism (e.g., protein, amino acid biosynthesis, and mitochondrial) genes (Fig. 2; see Tables S1 and S2 in the supplemental material), indicating high levels of metabolic activity in both species in the RHE. So given their differences in virulence in the RHE, it was surprising that growth initiation—as revealed by the temporal dynamics and magnitude of expression of the primary metabolism genes—appeared to be equally rapid in *C. albicans* and *C. dubliniensis*. Moreover, both species exhibited very similar upregulation in the RHE of C_2 utilization genes, such as genes for fatty acid β-oxidation, glyoxylate cycle, and gluconeogenesis, as well as heat shock protein genes (see Tables S5 and S6 in the supplemental material). This pattern of gene expression in mammalian tissues has previously been described only for *C. albicans* (46, 52), and upregulation of C_2 utilization and stress response genes also in *C. dubliniensis* suggests common pathways for physiological adaptation to the RHE environment in the two species. Thus, we hypothesize that only a small set of physiological cues in the RHE, triggering filamentation in *C. albicans* while failing to do so in *C. dubliniensis*, may be responsible for the difference in virulence. Filamentation of *C. albicans* cells growing on the polycarbonate filters used as RHE support matrix indicated

that hyphal morphogenesis in *C. albicans* was induced by the general RHE growth conditions, such as levels of CO_2 and composition of the media.

Our results indicated increased expression of many *C. albicans* virulence and hyphal genes, with lower or undetectable expression of these genes in *C. dubliniensis*. The use of the *C. albicans* microarray could have potentially underestimated the number of expressed genes in *C. dubliniensis*, including expression of several hyphal genes, where probes had lower specificity (<90% similarity) to the corresponding *C. dubliniensis* sequences (see Table S2 in the supplemental material). While we cannot exclude the possibility that the lack of detectable expression of these genes in *C. dubliniensis* was due to low probe-target similarity, the almost complete absence of hypha-associated gene expression in this species was consistent with its growth morphology and lower virulence in the RHE model.

Hyphal morphogenesis is a pivotal process for colonization and virulence in mucosal tissues by *C. albicans* (16, 26, 31) and some *C. dubliniensis* mutants (23). Accordingly, the reduction in RHE damage by the ΔΔ*sfl2* strains appeared to be due to their inability to form hyphae in this model (Fig. 7), as no effects on biomass in the RHE and growth rates of the ΔΔ*sfl2* strains were observed. Key events and genes for epithelial colonization have been identified in *C. albicans* (29, 52), but less is known about the factors that trigger filamentation in the RHE. CO_2 at concentrations present in the oral cavity (48) induce filamentation in *C. albicans*—but not in *C. dubliniensis* (23)—both *in vitro* (37) and in the RHE (14). As shown by Klengel and coworkers (14), CO_2/HCO_3^- directly stimulates activity of adenylyl cyclase for cyclic AMP (cAMP) production and hyphal morphogenesis in *C. albicans*. Therefore, it is noteworthy that apart from being unable to filament in the RHE, the ΔΔ*sfl2* strains were also impaired in CO_2-induced and microaerophilic (high-CO_2 and low oxygen) filamentation (Fig. 4 and 5). ΔΔ*sfl2* strains were still capable of forming germ tubes in 10% serum, although at a slightly reduced rate when no temperature shift was applied. Along with the RHE-PCF comparison, suggesting that *SFL2* expression does not specifically respond to contact with the epithelial cells but rather to the environmental culture conditions in the RHE infection model, our results suggest that the inability of the ΔΔ*sfl2* strains to colonize and damage the RHE was due to their failure to filament in response to the increased CO_2 levels or microaerophilic conditions in the RHE. Therefore, it appears that Sfl2 does not have a direct role in epithelial infection, but rather an indirect role in pathogenesis in the RHE model by virtue of its effect on hypha formation in response to CO_2 and microaerophilic conditions.

It is widely accepted that the ability to produce hyphae is an important virulence factor in *C. albicans*, supported by observations indicating that mutants that are defective in hyphal formation are usually less pathogenic *in vitro* than wild-type strains (16, 26, 31, 52). *SFL2* deletion had no detectable effect on survival in the mouse model of systemic infection. However, the finding that in the kidney tissues the ΔΔ*sfl2* cells grew almost exclusively in the yeast form was unexpected. This suggests that ΔΔ*sfl2* cells have a capacity to infect mice and affect mouse survival similar to wild-type cells, despite the fact that the ΔΔ*sfl2* strain does not produce hyphae in the kidney. The possibility that ΔΔ*sfl2* cells formed hyphae only during the early stages of infection and then reverted to the yeast form during the later stages was not supported by our data, which showed that ΔΔ*sfl2* strains grew only as yeast cells already at day 3 postinfection (Fig. 8). However, the possibility that ΔΔ*sfl2* cells might form hyphae prior to the 3-day time point cannot be discounted. Another possible reason for the lack of reduced virulence of ΔΔ*sfl2* strains in the mouse models might be that formation of hyphae was similar to WT *C. albicans* in organs other than the kidneys. The possibility that yeast cells alone can cause disease and death in mice is intriguing; however, confirmation of this awaits further testing in infection model experiments in which a range of organs are examined for fungal morphology and burdens as well as inflammatory responses during an infection time course. Although ΔΔ*sfl2* strains formed only yeasts or short filaments, there was significant immune cell infiltration associated with the renal lesions (Fig. 8) (data not shown). Since *Candida* virulence is correlated with the extent of immune cell infiltrate in the kidney (19), it is possible that the ΔΔ*sfl2* strain induces damage in the host similar to the WT and, hence, is similarly virulent. As infection outcome is determined by early renal immune responses in this infection model (19), it will be important in the future to examine the chemokine and cytokine responses to ΔΔ*sfl2* and WT strains.

Similarities of the inferred Sfl2 protein sequence to heat shock transcription factors and possession of a highly conserved heat-shock factor DNA-binding signature suggest that it may act as a transcriptional regulator. Sfl2p possesses sequence similarity, including the HSF-type DNA-binding domain, to Sfl1p, a nuclear protein involved in regulation of microaerophilic morphogenesis (3, 17). However, unlike *SFL2*, *SFL1* expression is constant across different conditions (17) and Sfl1p suppresses *C. albicans* hyphal morphogenesis under several conditions, including microaerophilic growth (3). This suggests that these two proteins possess opposing activities, but whether or not they interact has yet to be determined. Given that deletion of *SFL2* abrogated hyphal morphogenesis in response to increased CO_2 and shift to alkaline pH, Sfl2p may act downstream of the cAMP and pH morphogenesis pathways. Further studies are planned to investigate the roles of Sfl1p and Sfl2p in morphogenesis, including microarray analysis of single and double mutants and localization studies.

The lack of a CO_2 response in *C. dubliniensis* (23) makes it difficult to design experimental approaches to assign a role to the likely *SFL2* orthologue, *Cd36_55430*, in *C. dubliniensis*. While possession of a conserved HSF-type domain points to some overlap in structure between Sfl2p and Cd36_55430p, the remainder of the sequences showed only ~50% identity, and deletion of *Cd36_55430* gave no detectable effects on morphogenesis in *C. dubliniensis* CD36 in microaerophilic conditions (M.J.S., unpublished results). That expression of *SFL2* in *C. dubliniensis* triggered filamentation indicated that *SFL2* acts as a hyphal inducer also in this species. It further suggested that *SFL2* and its orthologue, *Cd36_55430*, either have functionally diverged or that *Cd36_55430* expression is repressed in *C. dubliniensis.* Repression of *Cd36_55430* under conditions that induce expression of *SFL2* is indeed supported by very low levels of expression in the RHE of *Cd36_55430* in *C. dubliniensis* compared to expression of *SFL2* in *C. albicans* (Fig. 3).

In conclusion, to our knowledge this study is the first that has compared global gene expression in *C. albicans* and *C. dub-*

liniensis in a model of oral infection. Using standard conditions for RHE infection, we have established a baseline comparison of gene expression in the two species in this important model and identified *SFL2* as a gene required for virulence in the RHE infection model. *SFL2* was significantly upregulated during the very early stages of RHE colonization, and its deletion drastically reduced filamentation and tissue damage of *C. albicans* in the RHE and also abolished filamentation in 5% CO_2, in response to pH, and in microaerophilic conditions. This, along with the relationship of the predicted Sfl2 protein to HSF-type DNA-binding transcription factors, suggests a role for Sfl2 as a regulator of filamentation and opens the way for detailed studies into the roles of Sfl2 in hyphal morphogenesis and *Candida* virulence.

ACKNOWLEDGMENTS

We thank Jan Walker at St. James's Hospital, Dublin, for fixation and staining of the RHE tissue sections; Joachim Morschhäuser, University of Würzburg, for supplying plasmid pSFS2A; and Arnaud Firon for the Gateway expression vector.

This work was supported by a grant from Science Foundation Ireland (Programme Investigator grant no. 04/IN3/B463) to D. Sullivan and grants from the European Commission to C. d'Enfert. (Galar Fungail 2 Marie Curie Research Training Network, MRTN-CT-2003-504148; FINSysB Marie Curie Initial Training Network, PITN-GA-2008-214004).

REFERENCES

1. **Al Mosaid, A., D. J. Sullivan, and D. C. Coleman.** 2003. Differentiation of *Candida dubliniensis* from *Candida albicans* on Pal's agar. J. Clin. Microbiol. **41:**4787–4789.
2. **Arnaud, M. B., M. C. Costanzo, M. S. Skrzypek, P. Shah, G. Binkley, C. Lane, S. R. Miyasato, and G. Sherlock.** 2007. Sequence resources at the Candida genome database. Nucleic Acids Res. **35:**D452–D456.
3. **Bauer, J., and J. Wendland.** 2007. *Candida albicans* Sfl1 suppresses flocculation and filamentation. Eukaryot. Cell **6:**1736–1744.
4. **Braun, B. R., M. V. Hoog, C. d'Enfert, M. Martchenko, J. Dungan, A. Kuo, D. O. Inglis, M. A. Uhl, H. Hogues, M. Berriman, M. Lorenz, A. Levitin, U. Oberholzer, C. Bachewich, D. Harcus, A. Marcil, D. Dignard, T. Iouk, R. Zito, L. Frangeul, F. Tekaia, K. Rutherford, E. Wang, C. A. Munro, S. Bates, N. A. Gow, L. L. Hoyer, G. Kohler, J. Morschhäuser, G. Newport, S. Znaidi, M. Raymond, B. Turcotte, G. Sherlock, M. Costanzo, J. Ihmels, J. Berman, D. Sanglard, N. Agabian, A. P. Mitchell, A. D. Johnson, M. Whiteway, and A. Nantel.** 2005. A human-curated annotation of the *Candida albicans* genome. PLoS Genet. **1:**36–57.
5. **Brown, D. H., A. D. Giusani, X. Chen, and C. A. Kumamoto.** 1999. Filamentous growth of *Candida albicans* in response to physical environmental cues and its regulation by the unique *CZF1* gene. Mol. Microbiol. **34:**651–662.
6. **Delbrück, S., and J. F. Ernst.** 1993. Morphogenesis-independent regulation of actin transcript levels in the pathogenic yeast *Candida albicans*. Mol. Microbiol. **10:**859–866.
7. **Dimopoulos, G., F. Ntziora, G. Rachiotis, A. Armaganidis, and M. E. Falagas.** 2008. *Candida albicans* versus *non-albicans* intensive care unit-acquired bloodstream infections: differences in risk factors and outcome. Anesth. Analg. **106:**523–529.
8. **Gilfillan, G. D., D. J. Sullivan, K. Haynes, T. Parkinson, D. C. Coleman, and N. A. R. Gow.** 1998. *Candida dubliniensis*: phylogeny and putative virulence factors. Microbiology **144:**829–838.
9. **Gillum, A. M., E. Y. H. Tsay, and D. R. Kirsch.** 1984. Isolation of the *Candida albicans* gene for orotidine-5′-phosphate decarboxylase by complementation of *S. cerevisiae URA3* and *Escherichia coli pyrF* mutations Mol. Gen. Genet. **198:**179–182.
10. **Hokamp, K., F. M. Roche, M. Acab, M. E. Rousseau, B. Kuo, D. Goode, D. Aeschliman, J. Bryan, L. A. Babiuk, R. E. W. Hancock, and F. S. L. Brinkman.** 2004. ArrayPipe: a flexible processing pipeline for microarray data. Nucleic Acids Res. **32:**W457–W459.
11. **Jackson, A. P., J. A. Gamble, T. Yeomans, G. P. Moran, D. Saunders, D. Harris, M. Aslett, J. F. Barrell, G. Butler, F. Citiulo, D. C. Coleman, P. W. J. de Groot, T. J. Goodwin, M. A. Quail, J. McQuillan, C. A. Munro, A. Pain, R. T. Poulter, M. A. Rajandream, H. Renauld, M. J. Spiering, A. Tivey, N. A. R. Gow, B. Barrell, D. J. Sullivan, and M. Berriman.** 2009. Comparative genomics of the fungal pathogens *Candida dubliniensis* and *C. albicans*. Genome Res. **19:**2231–2244.
12. **Jayatilake, J., Y. H. Samaranayake, L. K. Cheung, and L. P. Samaranayake.** 2006. Quantitative evaluation of tissue invasion by wild type, hyphal and SAP mutants of *Candida albicans*, and non-*albicans Candida* species in reconstituted human oral epithelium. J. Oral Pathol. Med. **35:**484–491.
13. **Jones, T., N. A. Federspiel, H. Chibana, J. Dungan, S. Kalman, B. B. Magee, G. Newport, Y. R. Thorstenson, N. Agabian, P. T. Magee, R. W. Davis, and S. Scherer.** 2004. The diploid genome sequence of *Candida albicans*. Proc. Natl. Acad. Sci. U. S. A. **101:**7329–7334.
14. **Klengel, T., W. J. Liang, J. Chaloupka, C. Ruoff, K. Schroppel, J. R. Naglik, S. E. Eckert, E. G. Mogensen, K. Haynes, M. F. Tuite, L. R. Levin, J. Buck, and F. A. Mühlschlegel.** 2005. Fungal adenylyl cyclase integrates CO_2 sensing with cAMP signaling and virulence. Curr. Biol. **15:**2021–2026.
15. **Lee, K. L., C. C. Campbell, and H. R. Buckley.** 1975. Amino-acid liquid synthetic medium for the development of mycelial and yeast forms of *Candida albicans*. J. Med. Vet. Mycol. **13:**148–153.
16. **Lermann, U., and J. Morschhäuser.** 2008. Secreted aspartic proteases are not required for invasion of reconstituted human epithelia by *Candida albicans*. Microbiology **154:**3281–3295.
17. **Li, Y., C. Su, X. Mao, F. Cao, and J. Chen.** 2007. Roles of *Candida albicans* Sfl1 in hyphal development. Eukaryot. Cell **6:**2112–2121.
18. **Liu, H. P., J. Kohler, and G. R. Fink.** 1994. Suppression of hyphal formation in *Candida albicans* by mutation of a *STE12* homolog. Science **266:**1723–1726.
19. **MacCallum, D. M., L. Castillo, A. J. P. Brown, N. A. R. Gow, and F. C. Odds.** 2009. Early-expressed chemokines predict kidney immunopathology in experimental disseminated *Candida albicans* infections. PLoS One **4:**e6420.
20. **Martinez, M., J. L. Lopez-Ribot, W. R. Kirkpatrick, B. J. Coco, S. P. Bachmann, and T. F. Patterson.** 2002. Replacement of *Candida albicans* with *C. dubliniensis* in human immunodeficiency virus-infected patients with oropharyngeal candidiasis treated with fluconazole. J. Clin. Microbiol. **40:**3135–3139.
21. **McManus, B. A., D. C. Coleman, G. Moran, E. Pinjon, D. Diogo, M. E. Bougnoux, S. Borecka-Melkusova, H. Bujdakova, P. Murphy, C. d'Enfert, and D. J. Sullivan.** 2008. Multilocus sequence typing reveals that the population structure of *Candida dubliniensis* is significantly less divergent than that of *Candida albicans*. J. Clin. Microbiol. **46:**652–664.
22. **Moran, G., C. Stokes, S. Thewes, B. Hube, D. C. Coleman, and D. Sullivan.** 2004. Comparative genomics using *Candida albicans* DNA microarrays reveals absence and divergence of virulence-associated genes in *Candida dubliniensis*. Microbiology **150:**3363–3382.
23. **Moran, G. P., D. M. MacCallum, M. J. Spiering, D. C. Coleman, and D. J. Sullivan.** 2007. Differential regulation of the transcriptional repressor *NRG1* accounts for altered host-cell interactions in *Candida albicans* and *Candida dubliniensis*. Mol. Microbiol. **66:**915–929.
24. **Morschhäuser, J., M. Ruhnke, S. Michel, and J. Hacker.** 1999. Identification of CARE-2-negative *Candida albicans* isolates as *Candida dubliniensis*. Mycoses **42:**29–32.
25. **Murad, A. M. A., P. R. Lee, I. D. Broadbent, C. J. Barelle, and A. J. P. Brown.** 2000. CIp10, an efficient and convenient integrating vector for *Candida albicans*. Yeast **16:**325–327.
26. **Naglik, J. R., D. Moyes, J. Makwana, P. Kanzaria, E. Tsichlaki, G. Weindl, A. R. Tappuni, C. A. Rodgers, A. J. Woodman, S. J. Challacombe, M. Schaller, and B. Hube.** 2008. Quantitative expression of the *Candida albicans* secreted aspartyl proteinase gene family in human oral and vaginal candidiasis. Microbiology **154:**3266–3280.
27. **Odds, F. C., M. F. Hanson, A. D. Davidson, M. D. Jacobsen, P. Wright, J. A. Whyte, N. A. R. Gow, and B. L. Jones.** 2007. One year prospective survey of *Candida* bloodstream infections in Scotland. J. Med. Microbiol. **56:**1066–1075.
28. **Odds, F. C., L. Van Nuffel, and G. Dams.** 1998. Prevalence of *Candida dubliniensis* isolates in a yeast stock collection. J. Clin. Microbiol. **36:**2869–2873.
29. **Park, H., Y. Liu, N. Solis, J. Spotkov, J. Hamaker, J. R. Blankenship, M. R. Yeaman, A. P. Mitchell, H. Liu, and S. G. Filler.** 2008. Transcriptional responses of *Candida albicans* to epithelial and endothelial cells. Eukaryot. Cell **8:**1488–1510.
30. **Park, Y. N., and J. Morschhäuser.** 2005. Tetracycline-inducible gene expression and gene deletion in *Candida albicans*. Eukaryot. Cell **4:**1328–1342.
31. **Phan, Q. T., P. H. Belanger, and S. G. Filler.** 2000. Role of hyphal formation in interactions of *Candida albicans* with endothelial cells. Infect. Immun. **68:**3485–3490.
32. **Phan, Q. T., C. L. Myers, Y. Fu, D. C. Sheppard, M. R. Yeaman, W. H. Welch, A. S. Ibrahim, J. E. Edwards, and S. G. Filler.** 2007. Als3 is a *Candida albicans* invasin that binds to cadherins and induces endocytosis by host cells. PLoS Biol. **5:**543–557.
33. **Pinjon, E., G. P. Moran, D. C. Coleman, and D. J. Sullivan.** 2005. Azole susceptibility and resistance in *Candida dubliniensis*. Biochem. Soc. Trans. **33:**1210–1214.
34. **Reuß, O., A. Vik, R. Kolter, and J. Morschhäuser.** 2004. The *SAT1* flipper, an optimized tool for gene disruption in *Candida albicans*. Gene **341:**119–127.
35. **Ritchie, M. E., J. Silver, A. Oshlack, M. Holmes, D. Diyagama, A. Holloway,**

and G. K. Smyth. 2007. A comparison of background correction methods for two-colour microarrays. Bioinformatics **23:**2700–2707.
36. **Schaller, M., K. Zakikhany, J. R. Naglik, G. Weindl, and B. Hube.** 2006. Models of oral and vaginal candidiasis based on in vitro reconstituted human epithelia. Nat. Protoc. **1:**2767–2773.
37. **Sims, W.** 1986. Effect of carbon dioxide on the growth and form of *Candida albicans*. J. Med. Microbiol. **22:**203–208.
38. **Slifkin, M.** 2000. Tween 80 opacity test responses of various *Candida* species. J. Clin. Microbiol. **38:**4626–4628.
39. **Smyth, G. K.** 2004. Linear models and empirical Bayes methods for assessing differential expression in microarray experiments. Stat. Appl. Genet. Mol. Biol. **3:**Article 3.
40. **Spiering, M. J., J. R. Faulkner, D.-X. Zhang, C. Machado, R. B. Grossman, and C. L. Schardl.** 2008. Role of the LolP cytochrome P450 monooxygenase in loline alkaloid biosynthesis. Fungal Genet. Biol. **45:**1307–1314.
41. **Stokes, C., G. P. Moran, M. Spiering, G. T. Cole, D. C. Coleman, and D. J. Sullivan.** 2007. Lower filamentation rates of *Candida dubliniensis* contribute to its lower virulence in comparison with *Candida albicans*. Fungal Genet. Biol. **44:**920–931.
42. **Sullivan, D. J., G. P. Moran, and D. C. Coleman.** 2005. *Candida dubliniensis*: ten years on. FEMS Microbiol. Lett. **253:**9–17.
43. **Sullivan, D. J., G. P. Moran, E. Pinjon, A. Al-Mosaid, C. Stokes, C. Vaughan, and D. C. Coleman.** 2004. Comparison of the epidemiology, drug resistance mechanisms, and virulence of *Candida dubliniensis* and *Candida albicans*. FEMS Yeast Res. **4:**369–376.
44. **Sullivan, D. J., T. J. Westerneng, K. A. Haynes, D. E. Bennett, and D. C. Coleman.** 1995. *Candida dubliniensis* sp. nov.: phenotypic and molecular characterization of a novel species associated with oral candidosis in HIV-infected individuals. Microbiology **141:**1507–1521.
45. **Thaweboon, S., B. Thaweboon, T. Srithavaj, and S. Choonharuangdej.** 2008. Oral colonization of *Candida* species in patients receiving radiotherapy in the head and neck area. Quintessence Int. **39:**E52–E57.
46. **Thewes, S., M. Kretschmar, H. Park, M. Schaller, S. G. Filler, and B. Hube.** 2007. In vivo and ex vivo comparative transcriptional profiling of invasive and non-invasive *Candida albicans* isolates identifies genes associated with tissue invasion. Mol. Microbiol. **63:**1606–1628.
47. **Tosello, M. E., M. S. Biasoli, A. G. Luque, H. M. Magaro, and A. R. Krapp.** 2007. Oxidative stress response involving induction of protective enzymes in *Candida dubliniensis*. Med. Mycol. **45:**535–540.
48. **Tsoukias, N. M., Z. Tannous, A. F. Wilson, and S. C. George.** 1998. Single-exhalation profiles of NO and CO_2 in humans: effect of dynamically changing flow rate. J. Appl. Physiol. **85:**642–652.
49. **Van Gelder, R. N., M. E. von Zastrow, A. Yool, W. C. Dement, J. D. Barchas, and J. H. Eberwine.** 1990. Amplified RNA synthesized from limited quantities of heterogenous cDNA. Proc. Natl. Acad. Sci. U. S. A. **87:**1663–1667.
50. **Wilson, R. B., D. Davis, and A. P. Mitchell.** 1999. Rapid hypothesis testing with *Candida albicans* through gene disruption with short homology regions. J. Bacteriol. **181:**1868–1874.
51. **Wong, L., and C. H. Sissions.** 2001. A comparison of human dental plaque microcosm biofilms grown in an undefined medium and a chemically defined artificial saliva. Arch. Oral Biol. **46:**477–486.
52. **Zakikhany, K., J. R. Naglik, A. Schmidt-Westhausen, G. Holland, M. Schaller, and B. Hube.** 2007. In vivo transcript profiling of *Candida albicans* identifies a gene essential for interepithelial dissemination. Cell. Microbiol. **9:**2938–2954.